De novo variants in *FRMD5* are associated with developmental delay, intellectual disability, ataxia, and abnormalities of eye movement

Graphical abstract

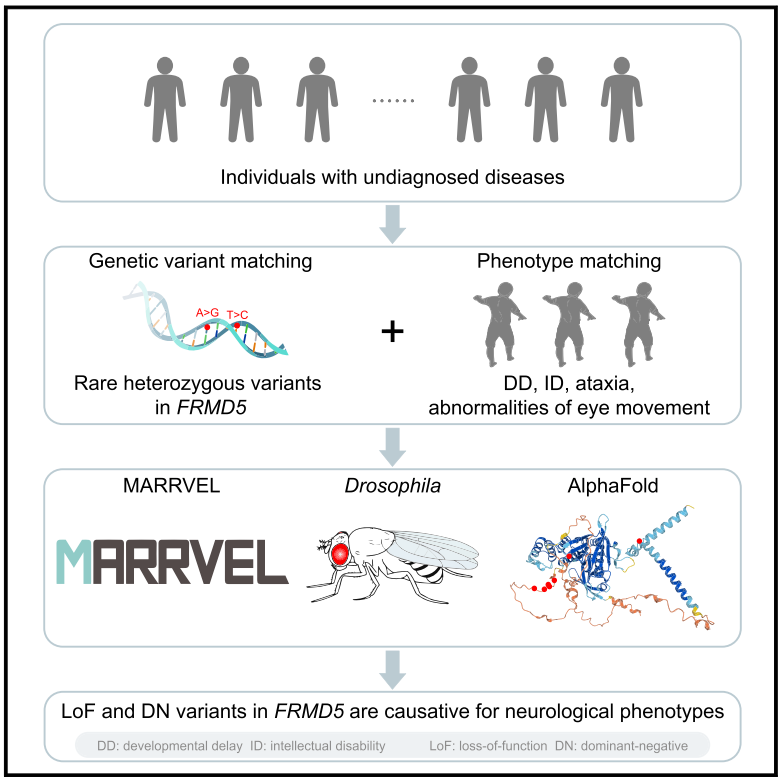

Authors

Shenzhao Lu, Mengqi Ma, Xiao Mao, ..., Michael F. Wangler, Yuwei Dai, Hugo J. Bellen

Correspondence

daiyuwei_1996@163.com (Y.D.), hbellen@bcm.edu (H.J.B.)

We report eight individuals with rare heterozygous variants in *FRMD5* who present with developmental delay, intellectual disability, ataxia and abnormalities of eye movement. Experimental evidence based on *Drosophila* studies and protein structure predictions indicate that these variants cause loss-of-function as well as dominant-negative effects.

Lu et al., 2022, The American Journal of Human Genetics *109*, 1932–1943
October 6, 2022
https://doi.org/10.1016/j.ajhg.2022.09.005

De novo variants in *FRMD5* are associated with developmental delay, intellectual disability, ataxia, and abnormalities of eye movement

Shenzhao Lu,[1,2] Mengqi Ma,[1,2] Xiao Mao,[3,4] Carlos A. Bacino,[1,5] Joseph Jankovic,[6] V. Reid Sutton,[1,5] James A. Bartley,[7] Xueying Wang,[8] Jill A. Rosenfeld,[1,9] Ana Beleza-Meireles,[10] Jaynee Chauhan,[11] Xueyang Pan,[1,2] Megan Li,[12] Pengfei Liu,[1,9] Katrina Prescott,[11] Sam Amin,[13] George Davies,[14] Michael F. Wangler,[1,2,5] Yuwei Dai,[3,15,*] and Hugo J. Bellen[1,2,16,*]

Summary

Proteins containing the FERM (four-point-one, ezrin, radixin, and moesin) domain link the plasma membrane with cytoskeletal structures at specific cellular locations and have been implicated in the localization of cell-membrane-associated proteins and/or phosphoinositides. FERM domain-containing protein 5 (FRMD5) localizes at cell adherens junctions and stabilizes cell-cell contacts. To date, variants in *FRMD5* have not been associated with a Mendelian disease in OMIM. Here, we describe eight probands with rare heterozygous missense variants in *FRMD5* who present with developmental delay, intellectual disability, ataxia, seizures, and abnormalities of eye movement. The variants are *de novo* in all for whom parental testing was available (six out of eight probands), and human genetic datasets suggest that *FRMD5* is intolerant to loss of function (LoF). We found that the fly ortholog of *FRMD5*, *CG5022 (dFrmd)*, is expressed in the larval and adult central nervous systems where it is present in neurons but not in glia. *dFrmd* LoF mutant flies are viable but are extremely sensitive to heat shock, which induces severe seizures. The mutants also exhibit defective responses to light. The human *FRMD5* reference (Ref) cDNA rescues the fly *dFrmd* LoF phenotypes. In contrast, all the *FRMD5* variants tested in this study (c.340T>C, c.1051A>G, c.1053C>G, c.1054T>C, c.1045A>C, and c.1637A>G) behave as partial LoF variants. In addition, our results indicate that two variants that were tested have dominant-negative effects. In summary, the evidence supports that the observed variants in *FRMD5* cause neurological symptoms in humans.

The FERM (four-point-one, ezrin, radixin, and moesin) domain is often located at the N terminus of FERM domain-containing proteins (FDCPs), linking the cytoskeletal network to the plasma membrane.[1] The FDCPs play important roles in cellular movements and migration by binding to a variety of proteins and lipids.[2] They contribute to membrane dynamics to mediate migration of the cell when responding to directional cues.[3,4] There are about 50 FDCPs in the human genome, and they participate in a variety of biological processes, such as wound healing and immune responses in health as well as cancer metastasis.[2] Fewer than 20 FDCPs have been reported to be associated with human diseases,[5] and the functions of the majority of the FDCPs remain to be discovered.

The FERM domain-containing protein 5 (*FRMD5* [MIM: 616309]) is localized to adherens junctions.[6] Previous studies have documented that knockdown of *FRMD5* promotes lung cancer cell migration and invasion.[6,7] FRMD5 inhibits migration through binding to integrin subunit beta 5 (ITGB5) and Rho-associated coiled-coil-containing protein kinase 1 (ROCK1).[7] However, other scientists showed that knockdown of *FRMD5* suppresses hepatocellular carcinoma cell (HCC) proliferation and tumorigenesis and that *FRMD5* is elevated by Wnt/β-catenin activation in human HCCs.[8] In addition, the transcriptional activity of *FRMD5* is regulated by β-catenin in colorectal cancer cells.[9] These data indicate different functional outcomes of loss of *FRMD5* in different contexts. However, variants in *FRMD5* have not been associated with a disease in the Online Mendelian Inheritance in Man (OMIM) database.[10]

We identified eight individuals with rare heterozygous missense *FRMD5* variants who present with neurodevelopmental disorders. Proper informed consent was obtained from legal guardians of the individuals. The variants are *de novo* in all the cases except for probands 7 and 8, for

[1]Department of Molecular and Human Genetics, Baylor College of Medicine, Houston, TX 77030, USA; [2]Jan and Dan Duncan Neurological Research Institute, Texas Children's Hospital, Houston, TX 77030, USA; [3]National Health Commission Key Laboratory for Birth Defect Research and Prevention, Hunan Provincial Maternal and Child Health Care Hospital, Changsha, Hunan 410008, China; [4]Department of Medical Genetics, Maternal and Child Health Hospital of Hunan Province, Changsha, Hunan 410008, China; [5]Texas Children's Hospital, Houston, TX 77030, USA; [6]Parkinson's Disease Center and Movement Disorders Clinic, Department of Neurology, Baylor College of Medicine, Houston, TX 77030, USA; [7]Loma Linda University Children's Hospital, Loma Linda, CA 92354, USA; [8]Department of Pediatrics, The Second Affiliated Hospital of Xi'an Jiaotong University, Xi'an, Shaanxi 710004, China; [9]Baylor Genetics Laboratories, Houston, TX 77021, USA; [10]Clinical Genetics Department, St Michael's Hospital, University Hospitals Bristol and Weston, Bristol BS1 3NU, UK; [11]Yorkshire Regional Genetics Service, Leeds Teaching Hospitals NHS Trust, Chapel Allerton Hospital, Leeds LS7 4SA, UK; [12]Invitae, San Francisco, CA 94103, USA; [13]Paediatric Neurology Department, Bristol Royal Pediatric Hospital, University Hospitals Bristol and Weston, Bristol BS1 3NU, UK; [14]University of Bristol, Bristol BS8 1QU, UK; [15]Department of Neurology, Xiangya Hospital, Central South University, Changsha, Hunan 410008, China; [16]Department of Neuroscience, Baylor College of Medicine, Houston, TX 77030, USA
*Correspondence: daiyuwei_1996@163.com (Y.D.), hbellen@bcm.edu (H.J.B.)
https://doi.org/10.1016/j.ajhg.2022.09.005.

whom the variants were not detected in maternal samples, but the paternal samples are unavailable. A summary of the clinical information, including nucleotide changes, of these probands can be found in Table 1. All probands exhibit developmental delay including motor delay. All probands present with intellectual disability, except proband 1, who is too young to be diagnosed. Seven probands have ataxia. They all exhibit abnormalities of eye movement. Among them, probands 2, 4, 5, and 7 have nystagmus, whereas probands 3, 6, and 7 have opsoclonus. Proband 1 has strabismus, and proband 8 has intermittent esotropia. Nystagmus and opsoclonus are abnormal involuntary eye movements, whereas strabismus is an abnormal conjugate eye movement. Five individuals have seizures, and proband 8 has an abnormal EEG. Some individuals have refractory seizures. Three of the eight individuals have abnormal brain MRIs (probands 2, 7, and 8). Proband 2 exhibited pachygyria in bilateral temporal lobes at the age of 6 (Figures 1A and 1B). For more detailed information, other symptoms, and other potential variants not within *FRMD5*, please see the case reports in the supplemental information.

To gather information on human *FRMD5* and the potential impact of the variants, we used the Model organism Aggregated Resources for Rare Variant ExpLoration (MARRVEL) tool,[11] which gathers information from multiple sources including Genome Aggregation Database (gnomAD[12]), OMIM, Database of Genomic Variants (DGV[13]), etc. *FRMD5* has a probability of loss-of-function (LoF) intolerance (pLI) score of 1.00 based on gnomAD,[12] suggesting that *FRMD5* may be a haploinsufficient gene and that loss of a single copy of the gene may cause the observed phenotypes. *FRMD5* has a missense *Z* score of 1.98, suggesting that *FRMD5* missense variants may not be tolerable.[14] However, there are few heterozygous LoF variants, and individuals with deletions that uncover *FRMD5* locus are observed in control[12,13] and disease datasets.[15,16] Together, these human population genetic data suggest that haploinsufficient or dominant-negative variants of *FRMD5* may create phenotypes.

Seven different missense variants in *FRMD5* (GenBank: NM_032892.5) were identified among the eight probands (c.1054T>C is shared by probands 4 and 5), and none of the variants are found in gnomAD. All the variants are predicted to be deleterious based on combined annotation dependent depletion (CADD) scores above 20 (Table 1).[17] Interestingly, five of the seven FRMD5 variants (p.Ser349-Arg, p.Ser351Gly, p.Ser351Arg, p.Cys352Arg, and p.Ser354-Pro) are clustered within very few amino acids (aa 349–354) in the FERM-adjacent (FA) domain, suggesting a hotspot region for *FRMD5*. Since DECIPHER[15] has not annotated any hotspot region for *FRMD5*, we queried MutScore,[18] a pathogenicity predictor, for region-specific constraint/missense variant analysis. There is no significant clustering for pathogenic or benign variants detected by MutScore (Figure S1). The MutLand plot from MutScore for *FRMD5* domains shows relatively higher scores for the FERM domain region (aa 21–354), suggesting that missense variants in this region are more likely to be pathogenic (Figure S1). The aa 530–555 region in the C terminus of the protein displays intermediate scores, while the aa 349–354 region does not show higher scores than the FERM domain region (Figure S1). In summary, little information is available about the aa 349–354 region of the FA domain.

Besides, there are two variants that map outside the aa 349–354 region: p.Phe114Leu maps to the FERM-middle (M) domain, whereas p.Tyr546Cys maps to the C terminus of the protein. There are two variants that are not confirmed to be *de novo*: p.Ser349Arg (maps to aa 349–354) and p.Tyr546Cys. Although p.Tyr546Cys maps to an uncharacterized region of the protein, the *in silico* data suggest that p.Tyr546Cys is deleterious, whereas the other variants observed in gnomAD with high frequencies are mostly predicted to be benign/tolerated (Table S1).

Drosophila dFrmd is an ortholog of *FRMD5*

To investigate the function of *FRMD5 in vivo*, we utilized *Drosophila* as the model organism.[19] The *Drosophila* RNAi Screening Center (DRSC) Integrative Ortholog Prediction Tool (DIOPT)[20] predicts one fly gene, *CG5022* (hereafter referred to as *dFrmd*), as the ortholog of both human *FRMD5* and *FRMD3*. The DIOPT score between *FRMD5* and *dFrmd* is 12 out of 16, suggesting a high level of homology between the two genes. The overall similarity and identity between FRMD5 and dFrmd are 47% and 33%, respectively (Figures 2A and S2), and the two proteins show similar domain topology, including the well-conserved FERM domain (Figure 2B). Taken together, these data indicate that fly *dFrmd* is orthologous to *FRMD5* in humans.

To study *FRMD5* in flies, we generated the fly reagents listed in Figure 2C and Table S2. These include a *CRISPR-Mediated Integration Cassette* (*CRIMIC*) allele of the *dFrmd* ($dFrmd^{CRIMIC\text{-}TG4}$),[21] which has a *Splice Acceptor (SA)-T2A-GAL4-polyA* cassette inserted in the first intron of the gene (Figure 2C). The $dFrmd^{CRIMIC\text{-}TG4}$ is likely a null allele, as it creates a truncated *dFrmd* mRNA (Figure 2D), and our real-time PCR data show that the $dFrmd^{CRIMIC\text{-}TG4}$ reduced the *dFrmd* mRNA levels to less than 1% (Figure 2E). This $dFrmd^{CRIMIC\text{-}TG4}$ allele also leads to the expression of *GAL4* under the endogenous gene-regulatory elements (Figure 2D) and allows us to assess the expression pattern of *dFrmd*, to explore LoF phenotypes, and to test the rescue ability of fly and human cDNAs.[21–23]

dFrmd is expressed primarily in neurons of the fly CNS

We first determined the expression pattern of *dFrmd* by crossing the $dFrmd^{CRIMIC\text{-}TG4}$ allele to *UAS-mCherry.NLS* (nuclear-localized mCherry fluorescent protein). The mCherry expression is obviously enriched in the larval central nervous system (CNS) (Figures 3A–3C). In both larval CNS and adult brain, mCherry (*dFrmd*) co-localizes with some Elav (pan-neuronal nuclear marker)-positive cells, but no obvious overlap was observed between mCherry and Repo (pan-glial nuclear marker) (Figures 3C

Table 1. Clinical features of affected individuals with *FRMD5* variants

Proband	1	2	3	4	5	6	7	8
Exome sequencing (ES)	Yes	Yes	Yes	Yes	Yes	Yes	Yes	Yes
FRMD5 variant (GenBank: NM_032892.5)	c.340T>C	c.1051A>G	c.1053C>G	c.1054T>C	c.1054T>C	c.1060T>C	c.1045A>C	c.1637A>G
Protein change	p.Phe114Leu	p.Ser351Gly	p.Ser351Arg	p.Cys352Arg	p.Cys352Arg	p.Ser354Pro	p.Ser349Arg	p.Tyr546Cys
CADD	29.1	23.3	22.6	23.6	23.6	27.8	23.4	26.3
Current age (years)	3	8	27	17	18	9	16	15.5
Inheritance	*de novo*	*de novo*	*de novo*	*de novo*	*de novo*	*de novo*	no paternal sample	no paternal sample
Age of onset	6 months	3 months	neonatal period	neonatal period	neonatal period	neonatal period	neonatal period	8 months
Sex	M	M	F	M	M	F	M	M
Motor delay	+	+++	+	+	++	+	+	++
Developmental delay	+	+++	+	+	++	+	+	++
Intellectual disability	N/A	+++	+ (borderline)	+	++	+	+	+
Seizures	++	+++	+	+	–	–	+	abnormal EEG
Ataxia	+	+	+	++	+	+++	+	–
Hypotonia	–	+	–	+	+	+	N/A	+
Spasticity	+	+	–	+	–	–	N/A	+
Abnormality of the eye	strabismus	nystagmus	opsoclonus	ocular vertical nystagmus/flutter	nystagmus, intermittent flutter with poor fixation, mild myopia, delayed visual maturation	opsoclonus, hypermetropia, visually impaired	nystagmus and opsoclonus	intermittent esotropia
Brain MRI	normal	pachygyria in bilateral temporal lobes	normal	normal	normal	normal	cystic foci in the periventricular white matter	delays in myelination
Additional features	feeding difficulties	feeding difficulties, severe constipation	myoclonus and dystonia; difficulty with fine motor skills; dyslexia; migraines	N/A	learning disability, behavioral problems, dystonia, dyskinetic and spasm-like movements and postures	moderate learning disability, urinary incontinence, behavior and self-regulation concerns, poor sleep, anxiety	learning problems, fatigue, headaches, interrupted sleep	ASD, renal anomalies

We report eight individuals with rare heterozygous variants in *FRMD5* who present with developmental delay, intellectual disability, ataxia, and abnormalities of eye movement. Experimental evidence based on *Drosophila* studies and protein structure predictions indicate that these variants cause loss-of-function as well as dominant-negative effects. CADD, combined annotation-dependent depletion; M, male; F, female; N/A, not available; EEG, electroencephalography; MRI, magnetic resonance imaging; ASD, autism spectrum disorder; –, +, ++, and +++, none, mild, moderate, and severe.

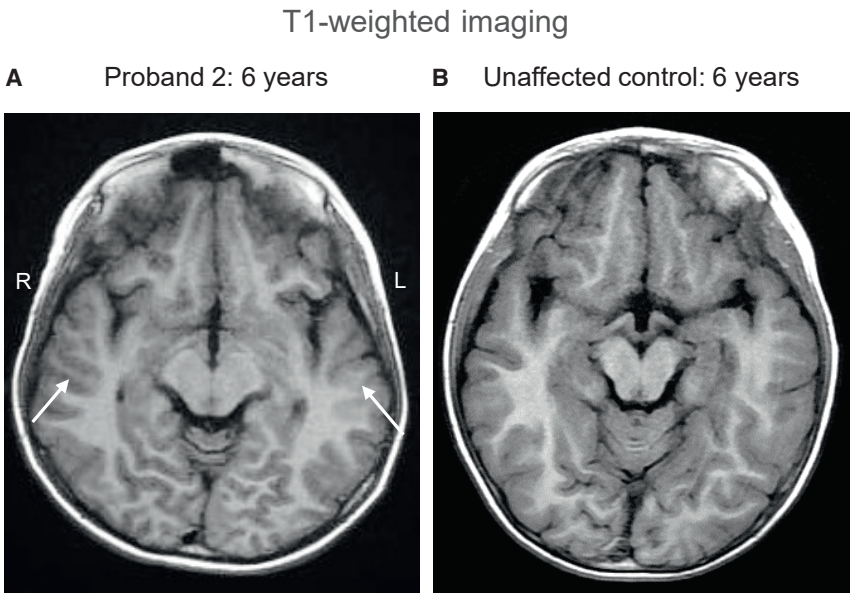

Figure 1. Brain MRI of proband 2
(A and B) Axial T1-weighted image from proband 2 at 6 years shows pachygyria in bilateral temporal lobes (A, white arrows), when compared to the unaffected control (B) of the same age and sex.

and 3D), indicating that *dFrmd* is mainly expressed in a subset of neurons, consistent with single-cell sequencing data.[24,25] To reveal the projections of *dFrmd*-expressing neurons, we used the $dFrmd^{CRIMIC\text{-}TG4}$ allele to drive *UAS-mCD8::RFP* (a membrane-bound red fluorescent protein). As shown in Figure 3E, RFP (*dFrmd*) labels neuropils of the central brain and ventral nerve cord in the larval CNS (Figure 3E). In the adult brain, RFP signals are observed in the optic lobes, antennal lobes, and mushroom bodies as well as other brain regions (Figure 3F). Altogether, these data show that *dFrmd* is specifically expressed in the neurons, in agreement with the prominent expression of *FRMD5* in the human CNS.[26]

Loss of *dFrmd* in flies causes heat-induced seizures and is rescued by the human *FRMD5* reference, but the variants rescue poorly

To explore the role of FRMD5 in the nervous system, we assessed phenotypes associated with *dFrmd* loss in flies. We generated *dFrmd* LoF mutant flies by crossing $dFrmd^{CRIMIC\text{-}TG4}$ to a deficiency (Df) line lacking *dFrmd*. The $dFrmd^{CRIMIC\text{-}TG4}$/Df mutants are viable and fertile and do not show obvious morphological abnormalities. Given that the probands exhibit seizures, we induced seizure-like behaviors in flies by mechanical stimulation (bang sensitivity assay)[27] or exposure to 42°C (heat shock assay).[28,29] The $dFrmd^{CRIMIC\text{-}TG4}$/Df mutants do not show obvious bang sensitivity but are very sensitive to heat shock, which induces severe seizures (Figures 4A and 4B). The mutant flies cannot climb properly and display wing fluttering, leg twitching, and abdominal muscle contractions (Video S1), and loss of *dFrmd* causes a slow recovery after heat shock (Figures S3A and S3B and Video S2). The heat-induced seizures are rescued by a genomic rescue (GR) construct that carries a copy of the *dFrmd* locus (Figures 2C, 4A, and S3A), indicating that the loss of *dFrmd* is the cause of the heat-sensitivity phenotype.

Next, we attempted to rescue the heat-induced seizures of *dFrmd* LoF mutants by expressing human *FRMD5* reference (Ref) or variant cDNAs. We generated the *UAS-dFrmd* wild-type (WT) and *UAS-FRMD5* transgenic fly lines and crossed them into the $dFrmd^{CRIMIC\text{-}TG4}$/Df background. Both the *UAS-dFrmd* WT and UAS-*FRMD5* Ref cDNA transgenes fully rescued the phenotype of *dFrmd* LoF mutants, at 25°C (Figure 4A) and 22°C (Figure 4B). In contrast, the three tested *FRMD5* variants exhibit significantly reduced rescue abilities when compared to the Ref (Figures 4A, 4B, and S3B), indicating that the tested *FRMD5* variants (c.1051A>G, c.1054T>C, and c.1637A>G) are partial LoF variants.

Loss of *dFrmd* in flies causes specific ERG defects

We also explored if FRMD5 affects synaptic transmission or phototransduction. We performed electroretinogram (ERG) recordings to assess the ability of the photoreceptors (PRs) to capture and transduce light signals and to assess if the PRs communicate properly with postsynaptic cells.[30,31] ERG recordings of the *dFrmd* LoF mutants did not show obvious defects at 10 days post-eclosion (Figure 4C) but started to show reduced On transients at 20–21 days (Figure 4D), and obviously decreased On and Off transients were observed in the *dFrmd* LoF mutants on day 30 (Figure 4E) when compared to the GR rescued flies. These data indicate that dFrmd is required to maintain proper synaptic transmission between the presynaptic photoreceptors and the postsynaptic lamina cells in an age-dependent manner. The On transient phenotype is fully rescued by expression of the *FRMD5* Ref cDNA, but the two variants that were tested (c.1051A>G and c.1637A>G) show significantly reduced rescue abilities (Figures 4F and 4G), again indicating that they are partial LoF variants.

Ectopic expression of human *FRMD5* Ref is toxic, whereas the variants are less toxic

To further investigate the nature of the *FRMD5* variants, we performed ectopic expression assays by expressing *UAS-FRMD5* cDNAs using different GAL4 drivers at different temperatures, as the GAL4 expression increases with temperature.[32,33] Interestingly, ubiquitous expression of *FRMD5* Ref using *daughterless-GAL4* (*da-GAL4*) causes semi-lethality at 18°C and full lethality at 22°C and 25°C

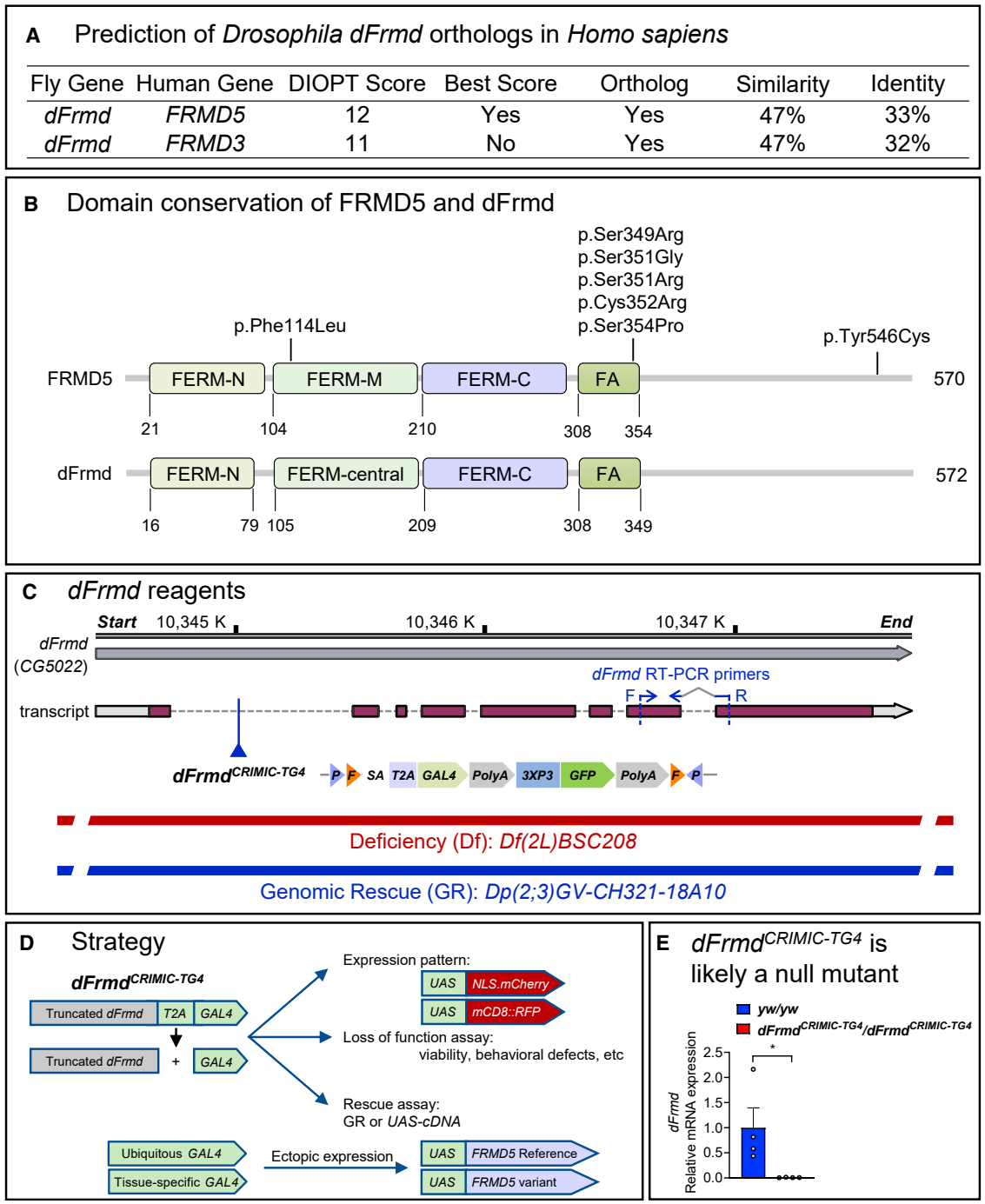

Figure 2. *CG5022* (*dFrmd*) is the *FRMD5* ortholog in fly

(A) *FRMD5* and *FRMD3* share the same fly ortholog, *dFrmd*. Data were obtained from DIOPT (DRSC Integrative Ortholog Prediction Tool).

(B) Protein domains are conserved between FRMD5 and dFrmd.

(C) Genomic structure of *dFrmd* locus and reagents used in this study. Real-time PCR primers to detect the *dFrmd* mRNA levels are also labeled.

(D) Strategy to study *FRMD5* in flies. Using $dFrmd^{CRIMIC\text{-}TG4}$, we determined the expression pattern and the loss-of-function (LoF) phenotypes and performed rescue assays. We also ectopically expressed *FRMD5* reference (Ref) and variants using different GAL4 drivers to assess their effects *in vivo*.

(E) Real-time PCR data show that $dFrmd^{CRIMIC\text{-}TG4}$ is a severe LoF or null mutant. Relative *dFrmd* mRNA expression levels in $dFrmd^{CRIMIC\text{-}TG4}$ mutant larvae decrease to <1% when compared to controls (*yw/yw*). Each dot represents an independent sample that contains 3–5 larvae. Data are represented as mean + SEM. Unpaired t tests. *$p < 0.05$.

(Figure S4A). Furthermore, the expression of *FRMD5* Ref using a wing-specific *nubbin-GAL4* (*nub-GAL4*) causes semi-lethality at 18°C and 22°C and full lethality at 25°C (Figures 5A and 5B), and the surviving flies show wing defects (Figure 5C). These data indicate that overexpression of *FRMD5* Ref is toxic in a dose-dependent manner. Similarly,

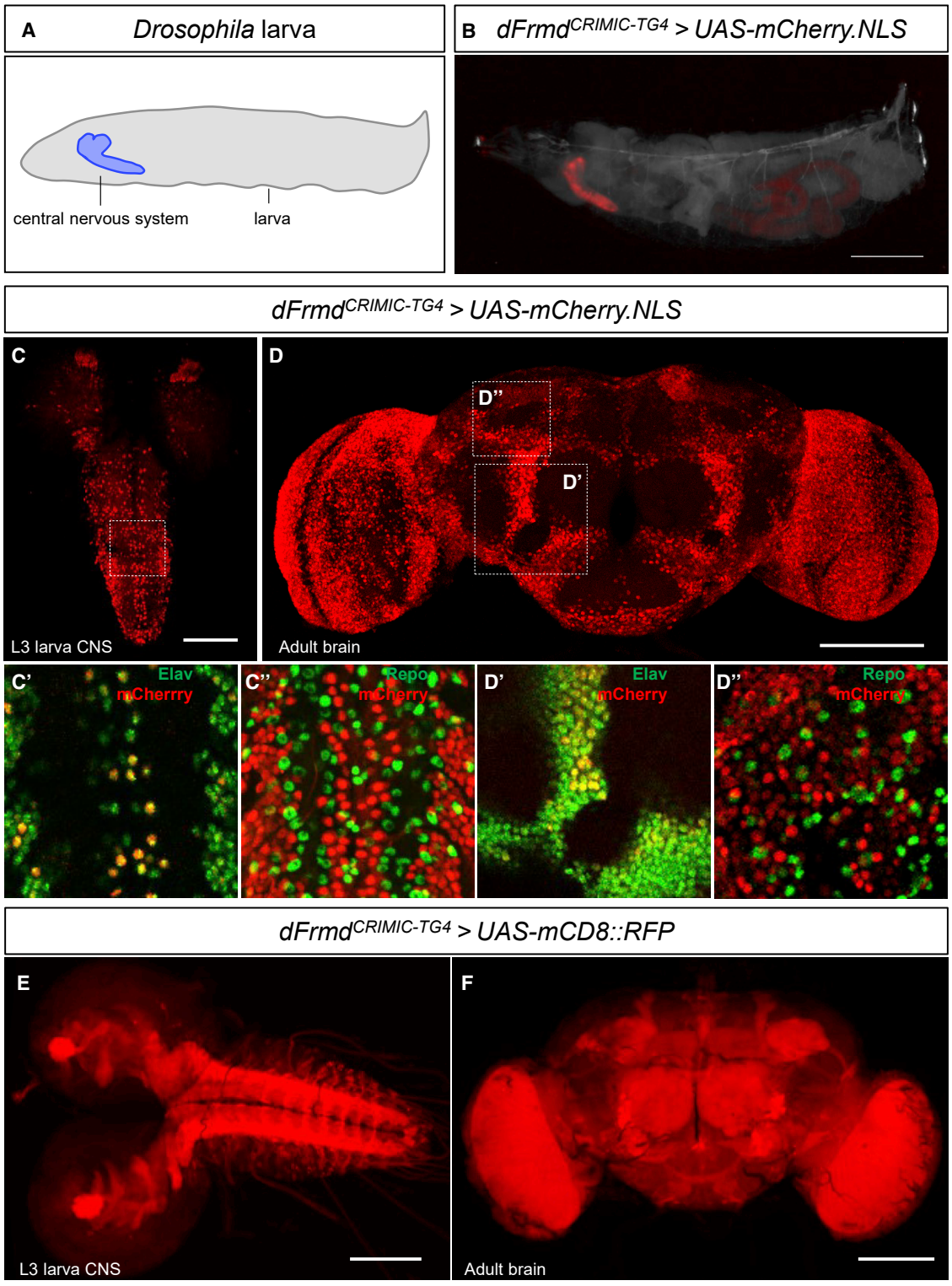

Figure 3. ***dFrmd*** **is expressed in neurons in the CNS**

(A) Schematic of the whole *Drosophila* larva highlighting the CNS.

(B) Expression pattern of *dFrmd* in whole third instar (L3) larva of the indicated genotype. Note that mCherry (*dFrmd*) is mainly expressed in the larval CNS. Scale bar, 1 mm.

(C and D) Expression pattern of *dFrmd* in the L3 larval CNS (C) and adult brain (D) is visualized using $dFrmd^{CRIMIC\text{-}TG4}$ allele-driven expression of *UAS-mCherry.NLS* co-stained with markers for neurons (Elav) or glia (Repo). Single-layer confocal images from the dashed squares indicate that mCherry is co-localized with Elav (C′, D′) but not Repo (C″, D″). Scale bars, 100 μm.

(E and F) The $dFrmd^{CRIMIC\text{-}TG4}$ allele-driven expression of *UAS-mCD8::RFP* (membrane-bound RFP) confirmed the broad expression of *dFrmd* in L3 larval CNS (E) and the adult brain (F). Scale bars, 100 μm.

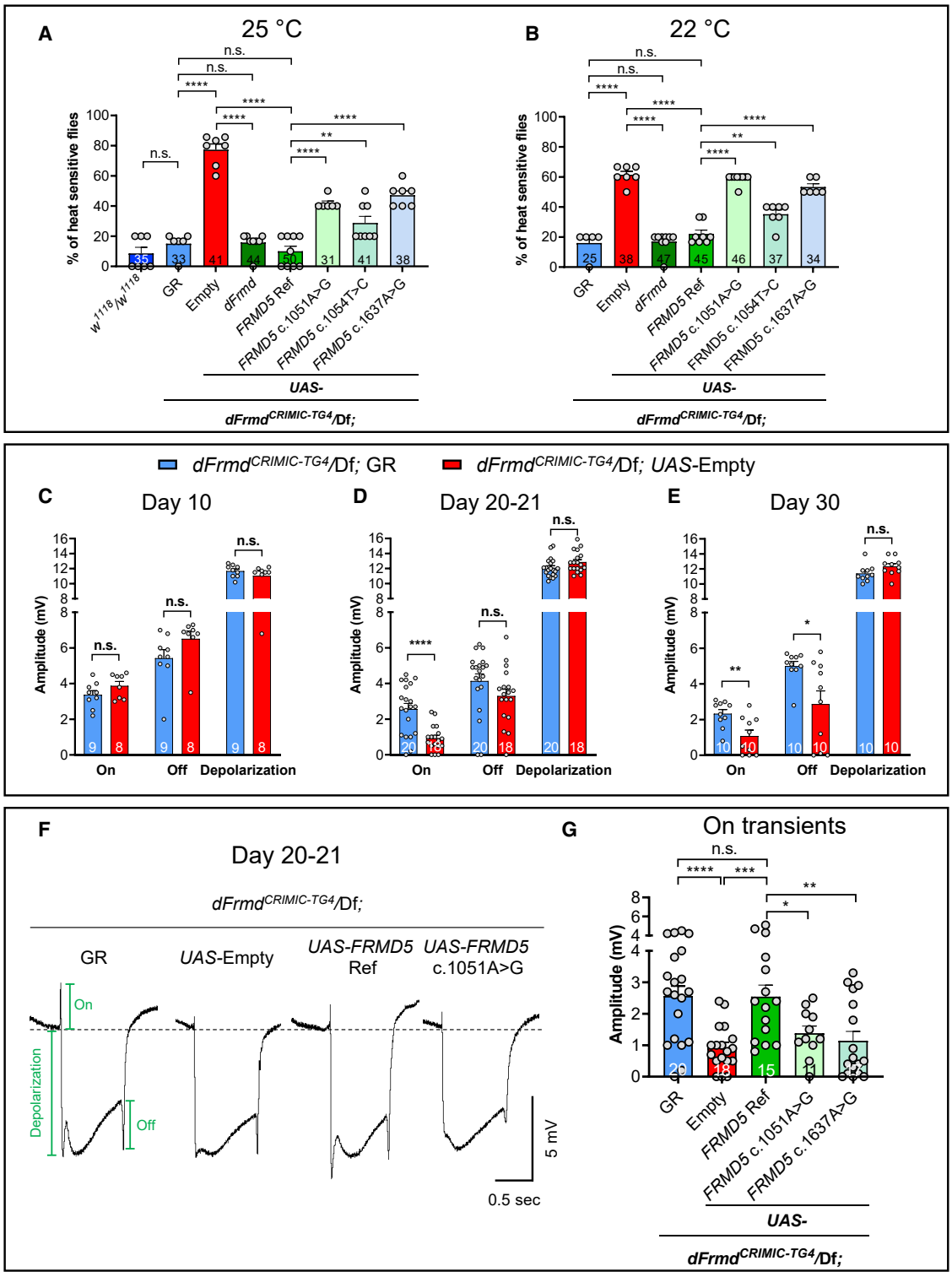

Figure 4. Loss of *dFrmd* in flies causes heat-induced seizures and specific ERG defects and is rescued by *FRMD5* reference but less so by the variants

(A and B) *dFrmd* LoF mutants exhibit heat-induced seizures. The percentage of *dFrmd* LoF mutant flies with seizures is significantly higher than controls (w^{1118}/w^{1118}) after exposure to a 42°C water bath for 30 s. The phenotype can be fully rescued with a genomic rescue (GR). The heat-induced seizures can be significantly rescued by fly *dFrmd* WT or human *FRMD5* Ref, but the human *FRMD5* variants have significantly reduced rescue abilities when compared to the Ref at 25°C (A) and 22°C (B). Flies were raised at 25°C (A) or 22°C (B) and tested at 14–15 days. Each dot represents an independent test of 5–8 flies.

(C–E) *dFrmd* LoF mutants show age-dependent ERG defects. The mutants do not show any ERG defect at day 10 (C), show decreased On transients at 20–21 days (D), and show decreased On and Off transients at day 30 (E). Flies were raised at 22°C.

(legend continued on next page)

overexpression of *dFrmd* WT using *da-GAL4* causes semi-lethality at 25°C (Figure S4A). Moreover, *nub-GAL4*-induced *dFrmd* WT expression causes wing defects at 25°C (Figures 5A and 5C). Six *FRMD5* variants (c.340T>C, c.1045A>C, c.1051A>G, c.1053C>G, c.1054T>C, and c.1637A>G) were tested, and they all showed decreased toxicity when compared to the Ref (Figures 5A, 5B, S4A, and S4B). When the Ref causes a toxic phenotype and the variants are less toxic, the variants are classified as LoF alleles.[22,34–40] In contrast, gain-of-function variants often cause more severe phenotypes in ectopic expression assays.[41] Hence, all assays that we carried out argue that the *FRMD5* variants are partial LoF variants. It's worth noting that the ectopic expression assays indicate that the c.1051A>G is the most severe variant, consistent with the human phenotype since proband 2 with the variant exhibits the most severe symptoms. Also, for the c.1637A>G that could not be confirmed to be *de novo*, the rescue assay and ectopic expression assays consistently show that it is a partial LoF allele.

FRMD5 variants disrupt the function of FRMD5 in a dominant-negative manner

A previous study showed that FRMD5 interacts with ROCK1 via the FA domain and inhibits the ROCK1 kinase activity.[7] Hence, FRMD5 regulates actin-based cytoskeletal remodeling by modulating the kinase activity of ROCK1.[7] Since the seven variants are missense, and five are clustered in the FA domain, these variants may disrupt FRMD5 function in a dominant-negative manner. To address if the variants are dominant negative, we expressed one copy of *FRMD5* Ref together with one copy of the *FRMD5* variants in the *dFrmd* LoF background ($dFrmd^{CRIMIC\text{-}TG4}$/Df). If a variant is a LoF variant, the expression of the *FRMD5* Ref should suppress the phenotype of the *dFrmd* LoF mutant, whereas the presence of a dominant-negative variant should reduce the rescue ability of the Ref.[42] As shown in Figure 5D, expression of the *FRMD5* Ref decreases the heat sensitivity from ~80% to ~20%. In contrast, co-expression of the Ref with either c.1051A>G or c.1054T>C causes an intermediate phenotype (Figure 5D). These data suggest that the tested variants impair the rescue ability of *FRMD5* Ref. These data indicate that the variants act in a dominant-negative manner.

Since the structure of the protein is fundamental for its function, we explored if the *FRMD5* variants lead to significant conformational changes in the protein when compared to the Ref. We predicted the three-dimensional structure of FRMD5 for the variants using the AlphaFold Protein Structure Database.[43,44] The variants in the FA domain are clustered in a loop (Figure S5A). Modeling based on AlphaFold did not show any obvious structural differences between the Ref and the variants, not only for the variants in the FA domain, but also for the two other variants (Figures S5B and S5D). Moreover, based on the ectopic expression assays, there are no significant functional differences between the variants clustering in the FA domain and the two variants that do not map to the FA domain (Figures 5B and S4B). These data suggest that all these variants may have dominant-negative effects.

Among the ~50 FDCPs, there are eight proteins with their names containing "FRMD" in human (FRMD1, 3, 4A, 4B, 5, 6, 7, and 8),[2,45] and two genes encoding FRMD4A and FRMD7 have been associated with human diseases. A homozygous frameshift mutation of the *FRMD4A* (MIM: 616305) in multiple affected individuals in a family is associated with severe neurologic symptoms, which include microcephaly and intellectual disability (MIM: 616819).[46] FRMD4A is a scaffolding protein that regulates epithelial cell polarity by connecting the small GTPase ADP-ribosylation factor 6 (ARF6) and the par-3 family cell polarity regulator (PARD3).[47] Suppression of *PARD3* (MIM: 606745) expression disrupts the polarity distribution of human neural progenitor cells.[48] Interestingly, the ankyrin repeat and LEM domain containing 2 (ANKLE2)-PAR complex pathway is conserved from flies to humans, and previous work showed that bi-allelic mutations in *ANKLE2* (MIM: 616062) are associated with microcephaly in humans.[49] Moreover, loss of *Ankle2* leads to loss of neuroblasts and disrupted asymmetric cell division of neuroblasts and causes microcephaly.[50]

Mutations in *FRMD7* (MIM: 300628) cause X-linked idiopathic congenital nystagmus (MIM: 310700).[51] FRMD7 is shown to activate GTPase RAC1 signaling *in vitro*[52] and co-localizes with actin in the growth cones of differentiated NEURO2A cells.[53] Knockdown of *FRMD7* during neuronal differentiation leads to disrupted actin cytoskeleton and results in altered neurite outgrowth.[53] However, little is known about the function of FRMD7 in animal models. Interestingly, the roundabout guidance receptor 1 (ROBO1), another protein localized to growth cones of neurons, controls axonal guidance in the *Drosophila* CNS,[54] and human individuals who are homozygous for LoF variants of *ROBO1* (MIM: 602430) exhibit nystagmus.[55]

It is striking that five of the seven *FRMD5* variants are clustered within very few amino acids (aa 349–354) in the FA domain. Although our knowledge about the structure and function of the FA domain is limited, a previous study showed that the FA domain of FRMD5 is required for FRMD5-ROCK1 interaction, and FRMD5 regulates actin-based cytoskeletal rearrangements by inhibiting the ROCK1 kinase activity.[7] Our data based on ERGs suggest that *dFrmd* is required to maintain proper synaptic

(F and G) The decreased On transients at 20–21 days can be rescued by human *FRMD5* Ref but not the variants. Representative ERG curves are shown in (F), and the quantitative data are shown in (G). Green annotations show the amplitude measurement of On/Off transients and depolarization. Flies were raised at 22°C.

For (A)–(E) and (G), total fly numbers are shown in the columns. Data are represented as mean + SEM. Unpaired t tests. *$p < 0.05$; **$p < 0.01$; ***$p < 0.001$; ****$p < 0.0001$; n.s., no significance.

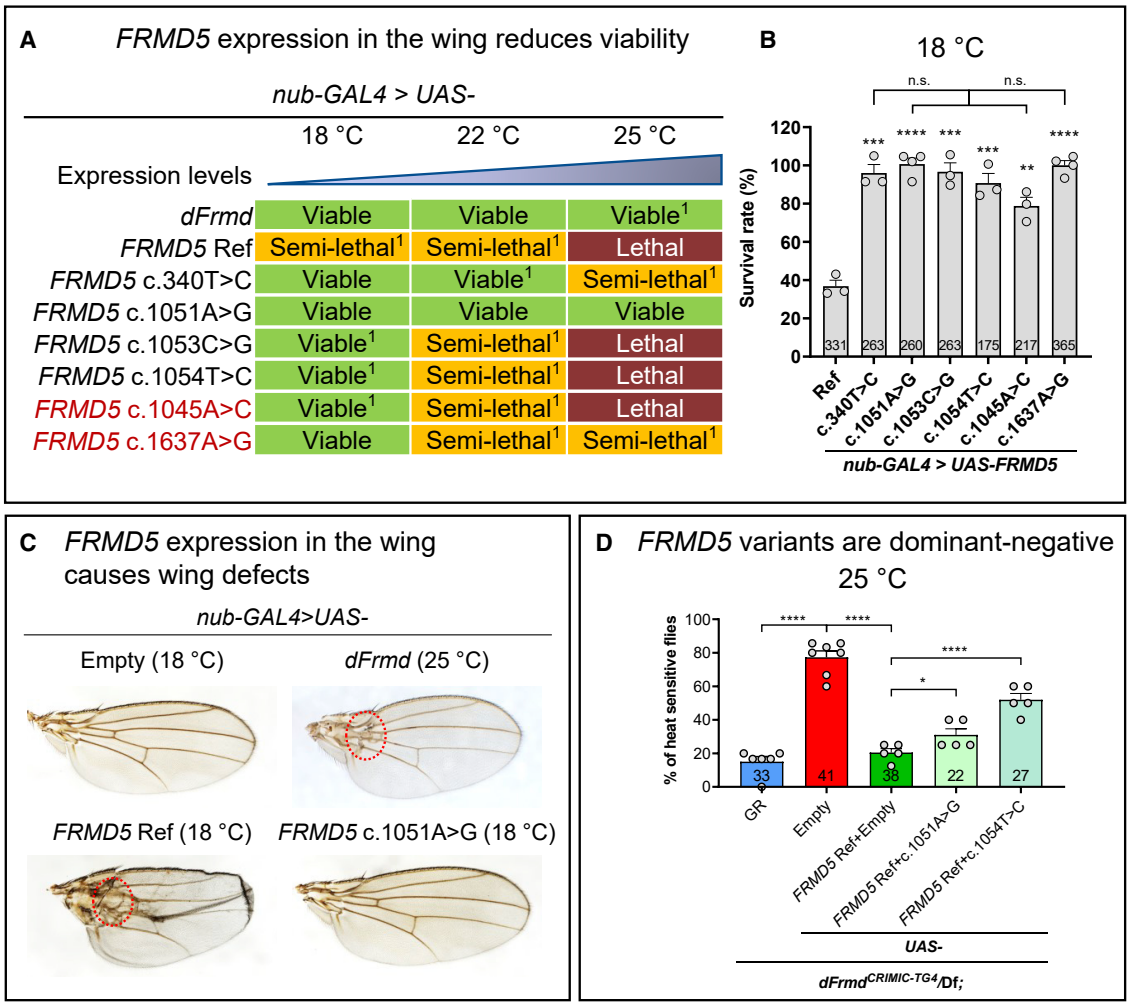

Figure 5. ***FRMD5*** **variants are less toxic, and some have dominant-negative effects**

(A) Summary of the lethality phenotype of wing-specific expression of *dFrmd*, *FRMD5* Ref, and variants at different temperatures. Note that the *FRMD5* Ref causes a more severe phenotype than the variants at 18°C. Some of the surviving flies exhibit wing defects and are noted as "[1]". The variants in red could not be confirmed to be *de novo*.

(B) Quantitative data at 18°C are shown. The survival rate is calculated when compared to *nub-GAL4>UAS*-Empty. Each dot represents an independent cross.

(C) Wing-specific overexpression of *dFrmd* and *FRMD5* Ref causes similar vein loss and blistery wing phenotypes. The defects are highlighted in red dashed circles.

(D) The heat shock assays for flies with $dFrmd^{CRIMIC\text{-}TG4}$ allele-driven expression of *FRMD5* cDNAs in the *dFrmd* LoF ($dFrmd^{CRIMIC\text{-}TG4}$/Df) background. The percentage of *dFrmd* LoF mutant flies with seizures was ~80% after exposure to a 42°C water bath for 30 s. The phenotype can be significantly rescued by human *FRMD5* Ref, but the tested *FRMD5* variants significantly reduced the rescue ability of *FRMD5* Ref. Flies were raised at 25°C and tested at 14–15 days. Each dot represents an independent test of 5–8 female flies.

For (B) and (D), total fly numbers are shown in the columns. Data are represented as mean + SEM. Unpaired t tests. *$p < 0.05$; **$p < 0.01$; ***$p < 0.001$; ****$p < 0.0001$; n.s., no significance.

transmission. Further studies examining the precise biological mechanisms will lead to a better understanding of the disease pathogenesis.

Data and code availability

All reagents developed in this study are available upon request. Some of the variants were submitted to ClinVar (GenBank: NM_032892.5): c.1053C>G, SCV002564145.1; c.1054T>C, SCV002564146.1; c.1045A>C, SCV002564147.1; c.1637A>G, SCV002564148.1. The exome datasets supporting this study have not been deposited in a public repository due to privacy and ethical/legal issues.

Supplemental information

Supplemental information can be found online at https://doi.org/10.1016/j.ajhg.2022.09.005.

Acknowledgments

We thank the probands and families for agreeing to participate in this study. We thank Ms. Hongling Pan for transgenic fly lines. We thank the Bloomington Drosophila Stock Center (BDSC) for numerous stocks and Drosophila Genomics Resource Center (DGRC, supported by NIH Grant 2P40OD010949) for the fly cDNA clone. We thank the Chigene (Beijing) Translational

Medicine Research Center Co. Ltd. for the technical support. This work was supported by the Howard Hughes Medical Institute (HHMI), the Huffington Foundation, and the Jan and Dan Duncan Neurological Research Institute at Texas Children's Hospital to H.J.B. Further support was obtained from The Office of Research Infrastructure Programs of the NIH (R24 OD022005 and R24 OD031447) to H.J.B. We thank the Deciphering Developmental Disorders (DDD) study for the referral of two probands. The DDD study presents independent research commissioned by the Health Innovation Challenge Fund (grant number HICF-1009-003). This study makes use of DECIPHER, which is funded by Wellcome (grant number 223718/Z/21/Z); see www.ddduk.org/access.html for full acknowledgement. This study makes use of data generated by the DECIPHER community. A full list of centers who contributed to the generation of the data is available from https://deciphergenomics.org/about/stats and via email from contact@deciphergenomics.org. We thank AlphaFold for structural predictions. The molecular graphics and analyses were performed with UCSF Chimera, developed by the Resource for Biocomputing, Visualization, and Informatics at the University of California, San Francisco, with support from NIH P41-GM103311. Please see the supplemental information for full acknowledgments.

Declaration of interests

The Department of Molecular and Human Genetics at Baylor College of Medicine receives revenue from clinical genetic testing completed at Baylor Genetics Laboratories. M.L. is a salaried employee and shareholder of Invitae Corp.

Received: April 14, 2022
Accepted: September 9, 2022
Published: October 6, 2022

Web resources

AlphaFold, https://alphafold.ebi.ac.uk/
CADD, https://cadd.gs.washington.edu/
DECIPHER, www.deciphergenomics.org
DGV, http://dgv.tcag.ca/dgv/app/home
DIOPT, https://www.flyrnai.org/diopt
gnomAD, http://gnomad.broadinstitute.org/
MARRVEL, http://www.marrvel.org/
MutScore, https://mutscore-wgt7hvakhq-ew.a.run.app/
OMIM, http://www.omim.org/
UCSF Chimera, https://www.rbvi.ucsf.edu/chimera/

References

1. Chishti, A.H., Kim, A.C., Marfatia, S.M., Lutchman, M., Hanspal, M., Jindal, H., Liu, S.C., Low, P.S., Rouleau, G.A., Mohandas, N., et al. (1998). The FERM domain: a unique module involved in the linkage of cytoplasmic proteins to the membrane. Trends Biochem. Sci. *23*, 281–282.
2. Bosanquet, D.C., Ye, L., Harding, K.G., and Jiang, W.G. (2014). FERM family proteins and their importance in cellular movements and wound healing (review). Int. J. Mol. Med. *34*, 3–12.
3. Frame, M.C., Patel, H., Serrels, B., Lietha, D., and Eck, M.J. (2010). The FERM domain: organizing the structure and function of FAK. Nat. Rev. Mol. Cell Biol. *11*, 802–814.
4. Patel, H., König, I., Tsujioka, M., Frame, M.C., Anderson, K.I., and Brunton, V.G. (2008). The multi-FERM-domain-containing protein FrmA is required for turnover of paxillin-adhesion sites during cell migration of Dictyostelium. J. Cell Sci. *121*, 1159–1164.
5. Amberger, J.S., and Hamosh, A. (2017). Searching Online Mendelian Inheritance in Man (OMIM): a knowledgebase of human genes and genetic phenotypes. Curr. Protoc. Bioinformatics *58*, 1.2.1–1.2.12.
6. Wang, T., Pei, X., Zhan, J., Hu, J., Yu, Y., and Zhang, H. (2012). FERM-containing protein FRMD5 is a p120-catenin interacting protein that regulates tumor progression. FEBS Lett. *586*, 3044–3050.
7. Hu, J., Niu, M., Li, X., Lu, D., Cui, J., Xu, W., Li, G., Zhan, J., and Zhang, H. (2014). FERM domain-containing protein FRMD5 regulates cell motility via binding to integrin beta5 subunit and ROCK1. FEBS Lett. *588*, 4348–4356.
8. Mao, X., Tey, S.K., Ko, F.C.F., Kwong, E.M.L., Gao, Y., Ng, I.O.L., Cheung, S.T., Guan, X.Y., and Yam, J.W.P. (2019). C-terminal truncated HBx protein activates caveolin-1/LRP6/beta-catenin/FRMD5 axis in promoting hepatocarcinogenesis. Cancer Lett. *444*, 60–69.
9. Zhu, C., Yamaguchi, K., Ohsugi, T., Terakado, Y., Noguchi, R., Ikenoue, T., and Furukawa, Y. (2017). Identification of FERM domain-containing protein 5 as a novel target of beta-catenin/TCF7L2 complex. Cancer Sci. *108*, 612–619.
10. Amberger, J.S., Bocchini, C.A., Schiettecatte, F., Scott, A.F., and Hamosh, A. (2015). OMIM.org: Online Mendelian Inheritance in Man (OMIM(R)), an online catalog of human genes and genetic disorders. Nucleic Acids Res. *43*, D789–D798.
11. Wang, J., Al-Ouran, R., Hu, Y., Kim, S.Y., Wan, Y.W., Wangler, M.F., Yamamoto, S., Chao, H.T., Comjean, A., Mohr, S.E., et al. (2017). MARRVEL: integration of human and model organism genetic resources to facilitate functional annotation of the human genome. Am. J. Hum. Genet. *100*, 843–853.
12. Karczewski, K.J., Francioli, L.C., Tiao, G., Cummings, B.B., Alföldi, J., Wang, Q., Collins, R.L., Laricchia, K.M., Ganna, A., Birnbaum, D.P., et al. (2020). The mutational constraint spectrum quantified from variation in 141, 456 humans. Nature *581*, 434–443.
13. MacDonald, J.R., Ziman, R., Yuen, R.K.C., Feuk, L., and Scherer, S.W. (2014). The Database of Genomic Variants: a curated collection of structural variation in the human genome. Nucleic Acids Res. *42*, D986–D992.
14. Lek, M., Karczewski, K.J., Minikel, E.V., Samocha, K.E., Banks, E., Fennell, T., O'Donnell-Luria, A.H., Ware, J.S., Hill, A.J., Cummings, B.B., et al. (2016). Analysis of protein-coding genetic variation in 60, 706 humans. Nature *536*, 285–291.
15. Firth, H.V., Richards, S.M., Bevan, A.P., Clayton, S., Corpas, M., Rajan, D., Van Vooren, S., Moreau, Y., Pettett, R.M., and Carter, N.P. (2009). DECIPHER: database of chromosomal imbalance and phenotype in humans using ensembl resources. Am. J. Hum. Genet. *84*, 524–533.
16. Landrum, M.J., Lee, J.M., Benson, M., Brown, G.R., Chao, C., Chitipiralla, S., Gu, B., Hart, J., Hoffman, D., Jang, W., et al. (2018). ClinVar: improving access to variant interpretations and supporting evidence. Nucleic Acids Res. *46*, D1062–D1067.
17. Rentzsch, P., Witten, D., Cooper, G.M., Shendure, J., and Kircher, M. (2019). CADD: predicting the deleteriousness of variants throughout the human genome. Nucleic Acids Res. *47*, D886–D894.

18. Quinodoz, M., Peter, V.G., Cisarova, K., Royer-Bertrand, B., Stenson, P.D., Cooper, D.N., Unger, S., Superti-Furga, A., and Rivolta, C. (2022). Analysis of missense variants in the human genome reveals widespread gene-specific clustering and improves prediction of pathogenicity. Am. J. Hum. Genet. *109*, 457–470.
19. Ma, M., Moulton, M.J., Lu, S., and Bellen, H.J. (2022). 'Fly-ing' from rare to common neurodegenerative disease mechanisms. Trends Genet. *38*, 972–984.
20. Hu, Y., Flockhart, I., Vinayagam, A., Bergwitz, C., Berger, B., Perrimon, N., and Mohr, S.E. (2011). An integrative approach to ortholog prediction for disease-focused and other functional studies. BMC Bioinf. *12*, 357.
21. Lee, P.T., Zirin, J., Kanca, O., Lin, W.W., Schulze, K.L., Li-Kroeger, D., Tao, R., Devereaux, C., Hu, Y., Chung, V., et al. (2018). A gene-specific T2A-GAL4 library for Drosophila. Elife *7*, e35574.
22. Lu, S., Hernan, R., Marcogliese, P.C., Huang, Y., Gertler, T.S., Akcaboy, M., Liu, S., Chung, H.L., Pan, X., Sun, X., et al. (2022). Loss-of-function variants in TIAM1 are associated with developmental delay, intellectual disability, and seizures. Am. J. Hum. Genet. *109*, 571–586.
23. Marcogliese, P.C., Deal, S.L., Andrews, J., Harnish, J.M., Bhavana, V.H., Graves, H.K., Jangam, S., Luo, X., Liu, N., Bei, D., et al. (2022). Drosophila functional screening of de novo variants in autism uncovers damaging variants and facilitates discovery of rare neurodevelopmental diseases. Cell Rep. *38*, 110517.
24. Davie, K., Janssens, J., Koldere, D., De Waegeneer, M., Pech, U., Kreft, Ł., Aibar, S., Makhzami, S., Christiaens, V., Bravo González-Blas, C., et al. (2018). A Single-Cell Transcriptome Atlas of the Aging Drosophila Brain. Cell *174*, 982–998.e20.
25. Li, H., Janssens, J., De Waegeneer, M., Kolluru, S.S., Davie, K., Gardeux, V., Saelens, W., David, F.P.A., Brbić, M., Spanier, K., et al. (2022). Fly Cell Atlas: A single-nucleus transcriptomic atlas of the adult fruit fly. Science *375*, eabk2432.
26. GTEx Consortium (2015). Human genomics. The Genotype-Tissue Expression (GTEx) pilot analysis: multitissue gene regulation in humans. Science *348*, 648–660.
27. Ganetzky, B., and Wu, C.F. (1982). Indirect Suppression Involving Behavioral Mutants with Altered Nerve Excitability in Drosophila melanogaster. Genetics *100*, 597–614.
28. Burg, M.G., and Wu, C.F. (2012). Mechanical and temperature stressor-induced seizure-and-paralysis behaviors in Drosophila bang-sensitive mutants. J. Neurogenet. *26*, 189–197.
29. Sun, L., Gilligan, J., Staber, C., Schutte, R.J., Nguyen, V., O'Dowd, D.K., and Reenan, R. (2012). A knock-in model of human epilepsy in Drosophila reveals a novel cellular mechanism associated with heat-induced seizure. J. Neurosci. *32*, 14145–14155.
30. Dolph, P., Nair, A., and Raghu, P. (2011). Electroretinogram recordings of Drosophila. Cold Spring Harb. Protoc. *2011*. pdb.prot5549.
31. Vilinsky, I., and Johnson, K.G. (2012). Electroretinograms in Drosophila: a robust and genetically accessible electrophysiological system for the undergraduate laboratory. J. Undergrad. Neurosci. Educ. *11*, A149–A157.
32. Duffy, J.B. (2002). GAL4 system in Drosophila: a fly geneticist's Swiss army knife. Genesis *34*, 1–15.
33. Nagarkar-Jaiswal, S., Lee, P.T., Campbell, M.E., Chen, K., Anguiano-Zarate, S., Cantu Gutierrez, M., Busby, T., Lin, W.W., He, Y., Schulze, K.L., et al. (2015). A library of MiMICs allows tagging of genes and reversible, spatial and temporal knockdown of proteins in Drosophila. Elife *4*, e05338.
34. Ansar, M., Chung, H.L., Al-Otaibi, A., Elagabani, M.N., Ravenscroft, T.A., Paracha, S.A., Scholz, R., Abdel Magid, T., Sarwar, M.T., Shah, S.F., et al. (2019). Bi-allelic variants in IQSEC1 cause intellectual disability, developmental delay, and short stature. Am. J. Hum. Genet. *105*, 907–920.
35. Kanca, O., Andrews, J.C., Lee, P.T., Patel, C., Braddock, S.R., Slavotinek, A.M., Cohen, J.S., Gubbels, C.S., Aldinger, K.A., Williams, J., et al. (2019). De Novo variants in WDR37 are associated with epilepsy, colobomas, dysmorphism, developmental delay, intellectual disability, and cerebellar hypoplasia. Am. J. Hum. Genet. *105*, 672–674.
36. Liu, N., Schoch, K., Luo, X., Pena, L.D.M., Bhavana, V.H., Kukolich, M.K., Stringer, S., Powis, Z., Radtke, K., Mroske, C., et al. (2018). Functional variants in TBX2 are associated with a syndromic cardiovascular and skeletal developmental disorder. Hum. Mol. Genet. *27*, 2454–2465.
37. Marcogliese, P.C., Shashi, V., Spillmann, R.C., Stong, N., Rosenfeld, J.A., Koenig, M.K., Martínez-Agosto, J.A., Herzog, M., Chen, A.H., Dickson, P.I., et al. (2018). IRF2BPL is associated with neurological phenotypes. Am. J. Hum. Genet. *103*, 245–260.
38. Ravenscroft, T.A., Phillips, J.B., Fieg, E., Bajikar, S.S., Peirce, J., Wegner, J., Luna, A.A., Fox, E.J., Yan, Y.L., Rosenfeld, J.A., et al. (2021). Heterozygous loss-of-function variants significantly expand the phenotypes associated with loss of GDF11. Genet. Med. *23*, 1889–1900.
39. Splinter, K., Adams, D.R., Bacino, C.A., Bellen, H.J., Bernstein, J.A., Cheatle-Jarvela, A.M., Eng, C.M., Esteves, C., Gahl, W.A., Hamid, R., et al. (2018). Effect of genetic diagnosis on patients with previously undiagnosed disease. N. Engl. J. Med. *379*, 2131–2139.
40. Uehara, T., Sanuki, R., Ogura, Y., Yokoyama, A., Yoshida, T., Futagawa, H., Yoshihashi, H., Yamada, M., Suzuki, H., Takenouchi, T., et al. (2021). Recurrent NFIA K125E substitution represents a loss-of-function allele: Sensitive in vitro and in vivo assays for nontruncating alleles. Am. J. Med. Genet. *185*, 2084–2093.
41. Goodman, L.D., Cope, H., Nil, Z., Ravenscroft, T.A., Charng, W.L., Lu, S., Tien, A.C., Pfundt, R., Koolen, D.A., Haaxma, C.A., et al. (2021). TNPO2 variants associate with human developmental delays, neurologic deficits, and dysmorphic features and alter TNPO2 activity in Drosophila. Am. J. Hum. Genet. *108*, 1669–1691.
42. Muller, H.J. (1932). Further studies on the nature and causes of gene mutations. Proc. 6th Int. Congr. Genet. *1*, 213–255.
43. Varadi, M., Anyango, S., Deshpande, M., Nair, S., Natassia, C., Yordanova, G., Yuan, D., Stroe, O., Wood, G., Laydon, A., et al. (2022). AlphaFold protein structure database: massively expanding the structural coverage of protein-sequence space with high-accuracy models. Nucleic Acids Res. *50*, D439–D444.
44. Jumper, J., Evans, R., Pritzel, A., Green, T., Figurnov, M., Ronneberger, O., Tunyasuvunakool, K., Bates, R., Žídek, A., Potapenko, A., et al. (2021). Highly accurate protein structure prediction with AlphaFold. Nature *596*, 583–589.
45. Moleirinho, S., Tilston-Lunel, A., Angus, L., Gunn-Moore, F., and Reynolds, P.A. (2013). The expanding family of FERM proteins. Biochem. J. *452*, 183–193.

46. Fine, D., Flusser, H., Markus, B., Shorer, Z., Gradstein, L., Khateeb, S., Langer, Y., Narkis, G., Birk, R., Galil, A., et al. (2015). A syndrome of congenital microcephaly, intellectual disability and dysmorphism with a homozygous mutation in FRMD4A. Eur. J. Hum. Genet. *23*, 1729–1734.
47. Ikenouchi, J., and Umeda, M. (2010). FRMD4A regulates epithelial polarity by connecting Arf6 activation with the PAR complex. Proc. Natl. Acad. Sci. USA *107*, 748–753.
48. Chen, X., An, Y., Gao, Y., Guo, L., Rui, L., Xie, H., Sun, M., Lam Hung, S., Sheng, X., Zou, J., et al. (2017). Rare Deleterious PARD3 variants in the apkc-binding region are implicated in the pathogenesis of human cranial neural tube defects via disrupting apical tight junction formation. Hum. Mutat. *38*, 378–389.
49. Yamamoto, S., Jaiswal, M., Charng, W.L., Gambin, T., Karaca, E., Mirzaa, G., Wiszniewski, W., Sandoval, H., Haelterman, N.A., Xiong, B., et al. (2014). A drosophila genetic resource of mutants to study mechanisms underlying human genetic diseases. Cell *159*, 200–214.
50. Link, N., Chung, H., Jolly, A., Withers, M., Tepe, B., Arenkiel, B.R., Shah, P.S., Krogan, N.J., Aydin, H., Geckinli, B.B., et al. (2019). Mutations in ANKLE2, a ZIKA virus target, disrupt an asymmetric cell division pathway in drosophila neuroblasts to cause microcephaly. Dev. Cell *51*, 713–729.e6.
51. Tarpey, P., Thomas, S., Sarvananthan, N., Mallya, U., Lisgo, S., Talbot, C.J., Roberts, E.O., Awan, M., Surendran, M., McLean, R.J., et al. (2006). Mutations in FRMD7, a newly identified member of the FERM family, cause X-linked idiopathic congenital nystagmus. Nat. Genet. *38*, 1242–1244.
52. Liu, Z., Mao, S., Pu, J., Ding, Y., Zhang, B., and Ding, M. (2013). A novel missense mutation in the FERM domain containing 7 (FRMD7) gene causing X-linked idiopathic congenital nystagmus in a Chinese family. Mol. Vis. *19*, 1834–1840.
53. Betts-Henderson, J., Bartesaghi, S., Crosier, M., Lindsay, S., Chen, H.L., Salomoni, P., Gottlob, I., and Nicotera, P. (2010). The nystagmus-associated FRMD7 gene regulates neuronal outgrowth and development. Hum. Mol. Genet. *19*, 342–351.
54. Kidd, T., Brose, K., Mitchell, K.J., Fetter, R.D., Tessier-Lavigne, M., Goodman, C.S., and Tear, G. (1998). Roundabout controls axon crossing of the CNS midline and defines a novel subfamily of evolutionarily conserved guidance receptors. Cell *92*, 205–215.
55. Huang, Y., Ma, M., Mao, X., Pehlivan, D., Kanca, O., Un-Candan, F., Shu, L., Akay, G., Mitani, T., Lu, S., et al. (2022). Novel dominant and recessive variants in human ROBO1 cause distinct neurodevelopmental defects through different mechanisms. Hum. Mol. Genet. *31*, 2751–2765.

The American Journal of Human Genetics, Volume *109*

Supplemental information

De novo variants in *FRMD5* are associated with developmental delay, intellectual disability, ataxia, and abnormalities of eye movement

Shenzhao Lu, Mengqi Ma, Xiao Mao, Carlos A. Bacino, Joseph Jankovic, V. Reid Sutton, James A. Bartley, Xueying Wang, Jill A. Rosenfeld, Ana Beleza-Meireles, Jaynee Chauhan, Xueyang Pan, Megan Li, Pengfei Liu, Katrina Prescott, Sam Amin, George Davies, Michael F. Wangler, Yuwei Dai, and Hugo J. Bellen

Supplemental Data

Supplemental note: case reports

Proband 1: c.340T>C (p.Phe114Leu)

This is a 3-year-old male with global developmental delay, drug-refractory epilepsy and ataxia. He did not have any exposure to alcohol or chemical substances during the prenatal period. His biological parents were healthy and non-consanguineous.

At the age of 6 months, he presented with frequent infantile spasms and absence seizures about 5-7 times per day, and was diagnosed with West syndrome. He was treated with topiramate and other anti-epilepsy drugs, but his seizures were not well controlled and he still had 1-2 seizures per month. At the age of ~2 years, he had another form of epileptic attack, manifesting as generalized tonic-clonic seizures and status epilepticus. The 24-hour continuous video electroencephalogram (EEG) at the age of 11 months demonstrated high amplitude spikes, sharp waves, and spike-slow complex discharges in the right frontal and temporal lobes. Brain MRI at the age of 2 years was normal. The head circumference is within normal limits.

Besides drug-refractory epilepsy, he had developmental delay in motor and verbal capabilities. He did not meet gross and fine motor developmental milestones in the first year of life. He could not stand up spontaneously or with assistance at the age of 1 year old. By the age of 3, he could stand up independently but was unable to walk independently. He also had a slow, wide-based gait using a walking aid. By the age of 3 years, he could not communicate using simple words. A recent physical evaluation found strabismus, hyperactive reflexes, normal muscle strength and tone throughout, and ataxia.

Trio exome sequencing (ES) detected a *de novo* missense variant in the candidate gene *FRMD5,* NM_032892.5 c.340T>C (p.Phe114Leu) that was confirmed by Sanger sequencing.

Proband 2: c.1051A>G (p.Ser351Gly)

This is a 9-year-old male with severe global developmental delay, refractory epilepsy and microcephaly. The prenatal and birth history were unremarkable. He was born at term with a birth weight of 3,600 g. At the age of 3 months, his family members began to notice that he could not raise his head; he also had a relatively small head circumference (39.0 cm, -1 SD by the age of 3 months). He has severe motor delay, demonstrated by the inability to stand and walk independently at the age of 8 years. He had poor motor coordination, especially in hand movement, and could not hold any objects. By the age of 8 years, he could not speak any simple words nor follow simple instructions. Neurologic examination shows muscular hypotonia, ataxia and horizontal nystagmus.

At the age of 3 months, he presented with infantile spasms and was diagnosed with West syndrome. The individual's mean seizure frequency ranges from 2-3 times to 30-50 times per day. Various anti-epilepsy drugs were used but the seizures were not well-controlled. At the age of 6 years, he began to receive sodium valproate, topiramate and clonazepam. With these treatments, he still has 3-5 seizures per month. At the age of 6 years, his EEG displayed interictal high amplitude spikes and 2-3 Hz spike-wave complexes in the bilateral frontotemporal area and the bilateral frontal lobe and occipital lobe. At the age of 6 years, MRI of the brain demonstrated pachygyria in bilateral temporal lobes.

Trio ES revealed a *de novo* missense variant in *FRMD5,* NM_032892.5, c.1051A>G (p.Ser351Gly), which was confirmed by Sanger sequencing.

Proband 3: c.1053C>G (p.Ser351Arg)

This 27-year-old woman of Jewish, Spanish, and Portuguese ancestry was initially evaluated at Baylor's Parkinson's Disease Center and Movement Disorders Clinic at the age of 15 years for a life-long history of jerking movements, gait and balance difficulty and abnormal eye movements. She is the product of an uncomplicated gestation and normal spontaneous vaginal

delivery. Her mother first noted abnormal eye movements at 2 weeks of age, initially diagnosed as nystagmus. The head circumference is within normal limits. MRI of the brain at age 3 months was normal. She had delayed developmental milestones; her first word was spoken at 18 months, but she spoke in full sentences at 2 years. She started to walk independently at age 3 years. Starting at six months of age when the individual had a fever, she developed brief spasms of her arms and legs, initially diagnosed as febrile seizures. Over time, however, these progressed to nearly continuous jerky movements affecting her upper and lower limbs, trunk and face. She has experienced occasional severe spasms of her entire body, lasting up to 20-45 minutes while completely awake. In addition, she has episodic cramping and inversion of her feet during which time she is unable to walk, especially in the afternoon and evening. She was initially suspected of having myoclonic epilepsy, but her EEG has been negative. She has always had an unsteady gait associated with frequent falls. She used a walker or wheelchair part of the time and required assistance when walking up and down stairs. Her myoclonus is worse with stress, fever and when hungry or fatigued. She has major difficulty with fine motor skills: difficulty with buttons, zippers, tying shoes and writing. She needs assistance with cutting and pouring liquids but is able to feed herself. In addition to her motor symptoms she has complained of numbness in legs and arms and hands, and she has started using a heating pad for 20 minutes to help recover her feeling. She is sensitive to hot and cold weather and feels her feet are "hot" when wearing shoes. She had difficulty with reading and math and was diagnosed with dyslexia. At the time of puberty she was diagnosed with migraines.

Gabapentin, baclofen and clonazepam have partly relieved her myoclonus and pain but she still has some “cramps” in her feet with flexion of the toes, especially when inactive. Levodopa slightly improved her gait and swallowing but was discontinued because of severe mood swings. Tetrabenazine caused severe drowsiness, and deutetrabenazine caused mood swings without improvement of her myoclonus. Her gabapentin dosages was recently increased to 600 mg 3x/day, along with baclofen 60 mg/day, and clonazepam 1.5 mg/day.

Her ES was done at Baylor Genetics in 2014, and trio ES was performed and analyzed at Invitae in 2019. The missense variant in *FRMD5,* NM_032892.5, c.1053C>G (p.Ser351Arg) (27/49 reads from the locus) was identified as a *de novo* variant. No other mutations or variants known to cause diseases were identified.

Proband 4: c.1054T>C (p.Cys352Arg)

This 17-year-old Saudi boy was evaluated at six years of age due to developmental delay and abnormal eye movements; he has had no follow-up since. He was a 3.67 kg product of a 41-week gestation delivered via Cesarean section for failure to progress, to a 42-year-old G5, P4>5, Ab0 L4>5 (G: gravida, P: para, Ab: abortions, L: living children) whose pregnancy was uncomplicated. On day of life #2 he was placed in the newborn intensive care unit because of shaking of legs and hands and abnormal movement of his eyes. He was treated with phenobarbital but this was stopped at 1.5 years of age, and these movements did not change after cessation of therapy. He had very low muscle tone early in life. He fed well (breastfed) with no problem. He received physical therapy, and parents reported that he continued to make improvement with his muscle tone and strength. He had a brain MRI that was reported to be normal although may have shown evidence of oxygen deprivation at birth. Other prior tesing was reported to have been normal (nerve conduction velocities of radialis and tibialis nerves, EEG, and biochemical testing, including plasma amino acid, urine organic acid, CSF neurotransmitter, urine oligosaccharide and lysosomal enzyme analyses). He had a stem cell transplant in China in 2011, and parents noted some improvement. Family history was remarkable for two paternal cousins (a girl and boy) with autism. Four older siblings were healthy and developmentally normal. There was no other family history of birth defects, intellectual disability or related problems. There was no family history or recurrent miscarriages. Parents are from Saudi Arabia. There is no known consanguinity.

He started crawling at 16 months, sitting up at age 2, and walking at age 5. His first word was at age 3 and was able to say sentences at 5 years. Physical examination at 6 years of age revealed weight at 98th centile, height at 61st centile and head circumference +2.05 SDs. He had vertical and possibly rotary nystagmus/flutter that was constant and did not change with closing eyelids nor with trying to fix on an object. There was a single hyperpigmented macule on the abdomen. He had central hypotonia with increased muscle tone in the right upper extremity. Gait was wide-based and ataxic. He did not have dysmorphic facial features or other differences noted on physical examination. ES was initially reported as non-diagnostic, but research re-analysis identified a *de novo* c.1054T>C (p.Cys352Arg) variant (64/147 reads from the locus) in *FRMD5* (NM_032892.5).

Proband 5: c.1054T>C (p.Cys352Arg)

The male proband was born 9 days overdue after a normal and uncomplicated pregnancy. A pendular nystagmus was evident from the first few days of life. He smiled socially at four weeks.

Global developmental delay has emerged around age 6 months. He had developmental delay at 2.5 years, and his head circumference was 48.5 cm. He was not walking, first crawling at 21 months. The proband walked unaided with an ataxic gait at 3 years. His language development was delayed, even when considering that he grew up in a bilingual household. He knew 50 words by 2.5 but was unable to formulate sentences. A marked pendular nystagmus was noted, with restricted upward gaze. The opthalmology examination was normal. All other cranial nerves were intact. He was found to be very hypotonic, but with no intention tremor or athetosis and normal reflexes. Power was 5/5 in all limbs. He was toilet trained at 6 years. At age 4 years, he had a wide vocabulary, although his words were quite unclear. His mother thought he was able to put perhaps five words together. He has some behavioral issues, in

particular anger in response to change. He can be oppositional at times. He has learning difficulties with an IQ around 70.

By the time he was 18 years old, his growth parameters were adequate, and he had no significant dysmorphism. He was walking with marked dyskinesia, intention tremor with dysmetria bilaterally and ataxia. The pendular nystagmus remains. He has hyperkinetic movements of his upper limbs, and hypermobility. Over the 16 years of follow up, it was not found to be a progressive condition.

Individual is the only child of a healthy and non-consanguineous White couple. There is no family history of any movement disorders, muscle disorders or developmental delay. His father had simple febrile convulsions as a toddler. He has a much older half-brother through his father who has dyslexia. His parents are separated, and he lives with his mother.

He was worked up for metabolic disease, chromosomal analysis, lactate determination, blood and urine amino acids and organic acids, and DNA analysis for Prader Willi Syndrome with no conclusive result except the noted genetic defect. He also had a muscle biopsy, EMG (electromyography) and nerve conduction studies to assess for any problems here. These were all normal. Two separate brain MRIs showed no abnormalities. Whole exome sequencing and whole genome sequencing have not identified a diagnosis, but research re-analysis identified a *de novo* c.1054T>C (p.Cys352Arg) variant in *FRMD5* (NM_032892.5).

Proband 6: c.1060T>C (p.Ser354Pro)

This is a 9-year-old girl with congenital opsoclonus, ataxia, hypotonia, learning difficulties, developmental delay and incontinence concerns. She is the only child to non-consanguineous parents, with no significant family history. She was born at term, following an uneventful pregnancy.

Abnormal eye movements were noted from birth by her parents, and she was diagnosed with congenital opsoclonus. She had extensive investigations into the cause for the opsoclonus

including metabolic tests, MRI brain, MIBG (a meta-iodobenzylguanidine scan), EEG and lumbar puncture, all of which were normal. She is now cared for by the visual impairment team. She also has hypermetropia requiring glasses for correction and has regular reviews by the orthoptist team.

She did not meet her developmental milestones. As a baby she had poor head control and was noted to be hypotonic. She began to crawl at 17 months. She began to walk with the use of aids at 2 years old. She walked with an unsteady broad gait and ataxia. Her balance and gait remain to be an issue with frequent falls and poor coordination. She uses a walker and a wheelchair. Her growth parameters including her head circumference were all in normal ranges.

Regarding her fine motor ability, she continues to struggle with a pincer grip at 9 years old. She had delays in her speech and language development, only starting to speak at 18 months old. At 3 years old she could make simple 3-word sentences. At 9 years old, she has slurred and slow speech and can confuse words. She has a moderate learning disability, currently attending a mainstream school with additional help. She is awaiting an autism assessment.

As a child it was noted that she had a prominent startle response. There was a query regarding the possibility of her suffering from absence seizures on the background of staring episodes. An EEG did not illustrate any abnormal findings. There have not been any seizure episodes queried after this early event.

She is on medication for sleeping and anxiety. Her behavior is an aspect which can be problematic with self-regulation issues. She remains under the care of pediatricians for urinary incontinence and is on desmopressin.

She was reviewed by clinical genetics at 2 years old. She had a CGH array which was normal and she was enrolled into a research study for developmental delay. The trio ES revealed a *de novo* c.1060T>C (p.Ser354Pro) variant in *FRMD5* (NM_032892.5).

Proband 7: c.1045A>C (p.Ser349Arg)

This is a 16-year-old male with ataxia, congenital nystagmus, atypical absence epilepsy and mild intellectual disability. He exhibited episodic abnormal eye movements since one week of age, deviation downward with a shaking of the eyes back and forth, with occasional bilateral arm shaking as well. Apgar scores were 8 and 9 at 1 and 5 minutes. His birth weight was 7 pounds 5 ounces, and there were no neonatal complications. Laboratory studies included normal electrolytes, normal CSF, normal video EEG, normal brain MRI, and normal abdominal imaging. Ophthalmology evaluation noted nystagmus and opsoclonus and recommended urine catecholamines, which were normal. Testing for mitochondrial disorders was normal. Evaluation for autoimmune encephalitis and pediatric neurotransmitter disease was normal. He had also had extensive testing for an inborn error of metabolism, which was negative. Prior seizure-like episodes were marked by staring for several seconds, upward eye rolling, or head dropping forward and to the side for up to several minutes. He had multiple eye rolling and staring episodes. In the past he was placed on Keppra, but this was discontinued due to side effects, and he has not been on any other anticonvulsant medications. His previous EEG was unremarkable as was an MRI study, but the REEG at the age of 8 showed a mildly abnormal EEG due to the presence of Occipital Intermittent Rhythmic Delta Activity (OIRDA) but became normal 2 months later. OIRDA has been noted to occur in association with generalized epilepsy.

He started sitting up at age 12 months, walked with a walker at age 5. His first word was at 12 months, but he is still difficult to understand, and he does not read or write. His head circumference was 57.2 cm at 12 years of age (within normal limits). The brain MRI at 4 years showed tiny cystic foci in the periventricular white matter of both cerebral hemispheres. These may represent remnants of cystic periventricular leukomalacia. The ventricles are normal in size. No mass effect, acute infarct or intracranial hemorrhage was seen. There was no developmental anomaly. The pituitary gland was normal with a T1 bright spot in the neurohypophysis. The corpus callosum, brainstem and cerebellum were normal. Spectroscopy

on the same day showed mild decreases in NAA (N-acetyl-aspartate) and mild increases in choline compared to age-matched control values. These findings were said to be non-specific and possibly related to brain development.

His current symptoms include fatigue, nystagmus, developmental delays, learning problems, headaches, seizures, staring spells, aggression, mood swings, memory problems, tics, spasms, walking problems (able to perform heel and toe walking but unable to perform tandem gait, casual gait mildly ataxic, unable to stand on either foot), interrupted sleep, and daytime sleepiness.

The ES revealed a rare heterozygous missense variant in *FRMD5*, NM_032892.5, c.1045A>C (p.Ser349Arg), which was confirmed by Sanger sequencing. It also revealed a variant of uncertain significance in *MFN2* (MIM: 608507): NM_014874.3, c.175G>T (p.Asp59Tyr), associated with autosomal dominant Charcot Marie Tooth disease type 2A. The mother was negative, and the father unavailable for testing.

Proband 8: c.1637A>G (p.Tyr546Cys)

This individual is a 15.5-year-old male who was initially evaluated by a clinical geneticist at age 2 years secondary to developmental delay and spasticity. He was noted to have delays at around 8 months of age as he was unable to complete his developmental milestones compared to his half-siblings. A brain MRI obtained at 2.5 years showed delays in myelination. An extensive evaluation for metabolic disorders was performed and was reported as normal including lactate acid, ammonia, acylcarnitine profile, creatine and guanidinoacetate levels, orotic acid, plasma amino acids and urine organic acids. Chromosome studies and chromosome microarray were normal. Fragile X testing was also normal. ES at 7 years of age was only remarkable for a heterozygous variant of uncertain significance (VUS) in *KMT2C* (MIM: 606883): NM_170606.2, c.13534C>A (p.His4512Asn). Pathogenic variants in this gene have been found in individuals with Kleefstra syndrome (MIM: 617768) who do not have *EHMT1*

(MIM: 607001) variants. The clinical presentation was not suggestive for Kleefstra syndrome however. A further ES review showed a variant in *FRMD5* c.1637A>G (p.Tyr546Cys), which was confirmed by Sanger sequencing. The VUS in *KMT2C* and the *FRMD5* variant were not found in his mother, and the father was not available for testing.

The development was his main area of concern and significant for moderate to severe global delay. He started crawling at age 2.5 years, walked at 4 years and was late developing overall. He had toe walking due to spasticity. He had limited speech and was only able to say a few words. Attends a special education program and receives ABA (applied behavior analysis) therapy secondary to a diagnosis of autism. Family history was noncontributory. His mother had two sons and a daughter from a previous marriage, who are healthy. There no one else in the family with similar symptoms.

At age 11 years he was evaluated by neurology due to a movement disorder with frequent grimacing, neck extension, hand wringing, self-hugging, and anxiety with strangers. He also had bruxism. He has been followed by gastroenterology and nutrition secondary to suboptimal growth. He had appropriate growth early in infancy, but length and weight starting lagging at 8-10 months of age despite adequate nutrition. He eats well and has no constipation although has regurgitation and rumination behaviors. He is followed by the renal service because of horseshoe kidneys and mild hydronephrosis. At 10 years of age his EEG was abnormal due to the presence of rare spike activity in the right central region. This finding indicates the presence of a focal potentially epileptogenic process in this region. No electrical seizures recorded.

His last physical exam was done at 13.5 years. His height was 134.3 cm (Z= -3.05) and weight 29.8 kg (Z= -2.78), all below normal parameters according to CDC growth curves. His head circumference was 53.4 cm (26th percentile using Nelhaus growth chart). He has no dysmorphic features. His neurological exam was normal for cranial nerves and deep tendon reflexes. He displayed several repetitive movements and behaviors including shaking of the

head, neck extension, self-hugging, wringing of the hands and some hand flapping. He also had bruxism. The gait stance was unusual with slight flexion of the knees. Genitourinary exam was normal with Tanner stage II. The skin was very dry and thick on his hands and dry in the inner aspect of his feet. The rest of the exam was unremarkable.

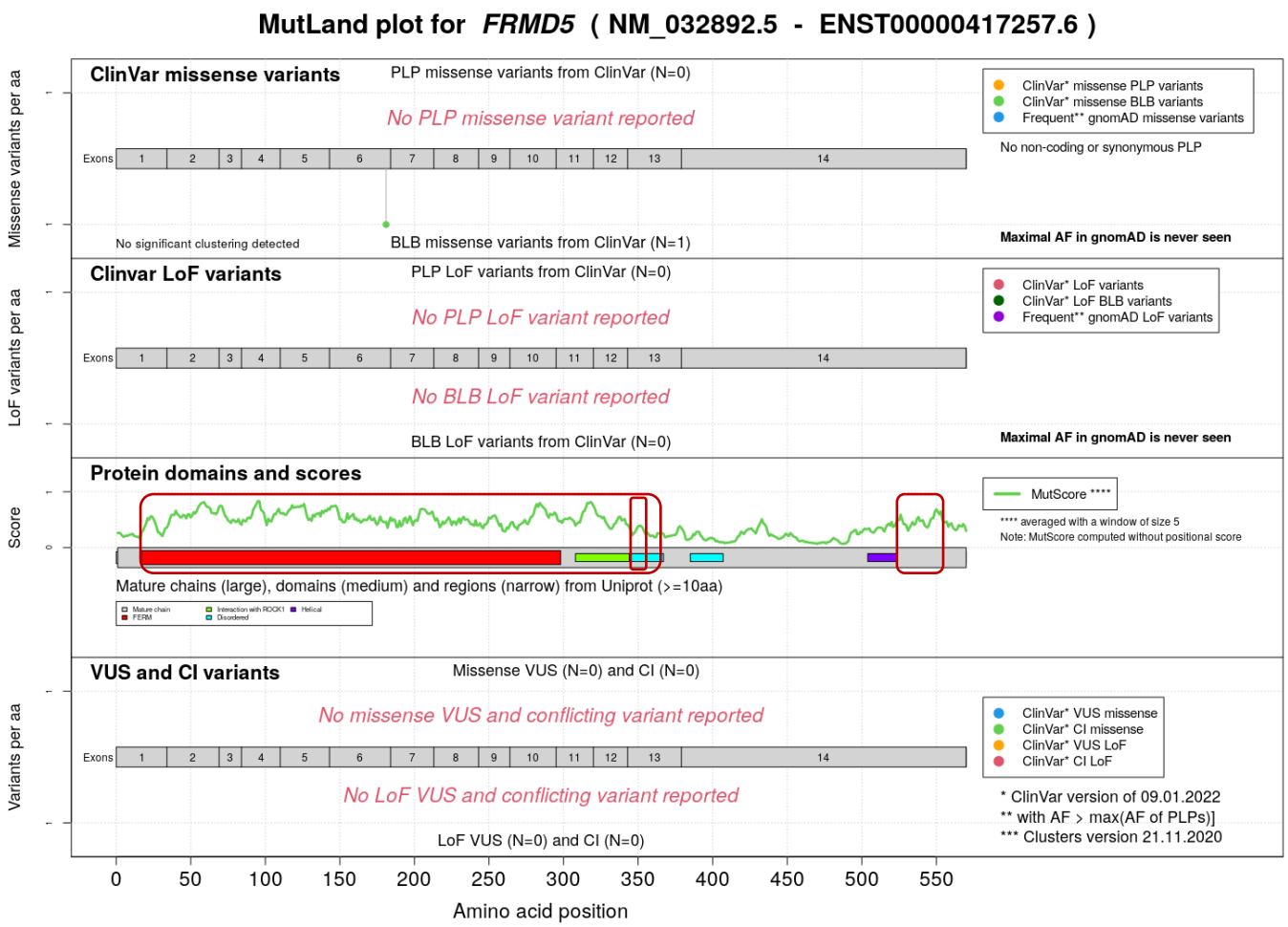

Figure S1. Visual presentation of MutScore prediction for *FRMD5*

The MutLand graphical output for *FRMD5*. No pathogenic and likely pathogenic (PLP) variants were detected. One variant, c.542C>T (p.Thr181Met), is shown as a benign and likely benign (BLB) variant. For more information of this variant please see Table S1. The predicted scores are averaged with a window size of 5. The regions of the protein mentioned in the text are highlighted with red boxes. Among them, the FERM domain region (AA 21-354) shows high scores, suggesting that missense variants in this region are more likely to be pathogenic. The AA 530-555 region in the C-terminus of the protein shows intermediate scores. For more information of p.Tyr546Cys variant please see Table S1. The clustering region (AA 349-354) does not show higher scores. No variants of uncertain significance (VUS) and conflicting interpretation (CI) variants were reported before July, 2022.

Figure S2. Protein sequence alignment of *Homo sapiens* FRMD5 and *Drosophila* dFrmd

Alignment of FRMD5 and dFrmd. Among the seven variants identified, three variants labeled in green color are at conserved amino acids (p.Ser351Gly, p.Ser351Arg, and p.Tyr546Cys). Protein isoforms for alignment: *Homo sapiens* FRMD5: NP_116281.2; *Drosophila* dFrmd: NP_609384.1. Similarity: 47%; Identity: 33%. Symbols in the protein alignment: identical (|), similar (:), different (.), absent (–). Data are from DIOPT.

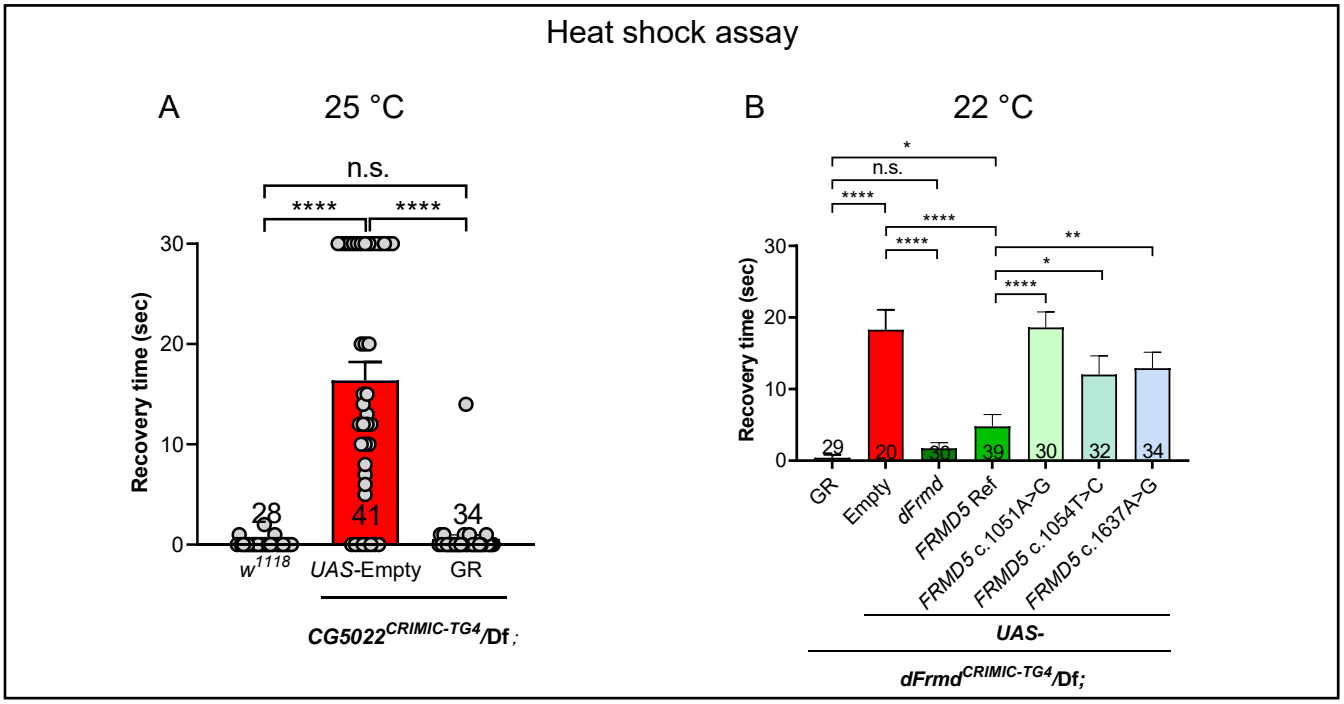

Figure S3. Loss of *dFrmd* in flies causes slow recovery after heat shock, and is rescued by *FRMD5* reference but less so by the variants

(**A**) *dFrmd* LoF mutant flies show slow recovery from seizures when compared to controls (w^{1118}/w^{1118}) after 42 °C water bath for 30 seconds. The phenotype can be fully rescued using a genomic rescue (GR) line. Flies were raised at 25 °C and tested at 14-15 days. Data are represented as mean + SEM. Unpaired t tests. ****P < 0.0001; n.s., no significance.

(**B**) The slow recovery after heat shock can be significantly rescued by fly *dFrmd* WT or human *FRMD5* Ref, but the human *FRMD5* variants have significantly reduced rescue abilities when compared to the Ref. Flies were raised at 22 °C and tested at 14-15 days. Data are represented as mean + SEM. Unpaired t tests. *P < 0.05; **P < 0.01; ****P < 0.0001; n.s., no significance.

A Ubiquitous *FRMD5* expression reduces viability

da-GAL4 > UAS-

Expression levels	18 °C	22 °C	25 °C
dFrmd	Viable	Viable	Semi-lethal
FRMD5 Ref	Semi-lethal	Lethal	Lethal
FRMD5 c.340T>C	Viable	Lethal	Lethal
FRMD5 c.1051A>G	Viable	Viable	Viable
FRMD5 c.1053C>G	Viable	Lethal	Lethal
FRMD5 c.1054T>C	Viable	Lethal	Lethal
FRMD5 c.1045A>C	Viable	Lethal	Lethal
FRMD5 c.1637A>G	Viable	Lethal	Lethal

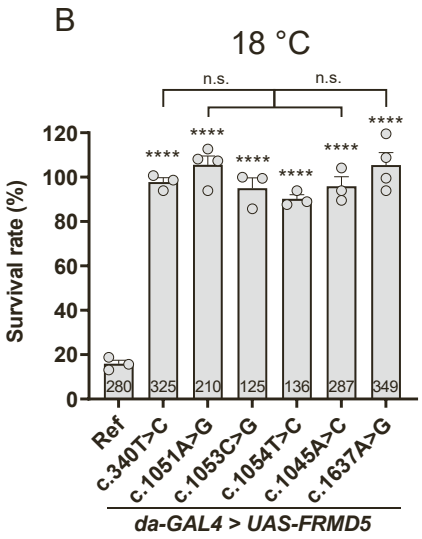

Figure S4. Ectopic expression of human *FRMD5* Ref is toxic, but the human *FRMD5* variants are less toxic

(**A**) Table summarizing the lethality phenotype of ubiquitous expression of *dFrmd*, *FRMD5* Ref and variants using *da-GAL4* at different temperatures. Note that the *FRMD5* Ref causes a more severe phenotype than the variants at 18 °C. The variants in red color could not be confirmed to be *de novo*. (**B**) Quantitative data at 18 °C are shown. The survival rate is calculated when compared to *da-GAL4>UAS-Empty*. Each dot represents an independent cross. Total fly numbers are shown in the columns. Data are represented as mean + SEM. Unpaired t tests. ****$P < 0.0001$; n.s., no significance.

A

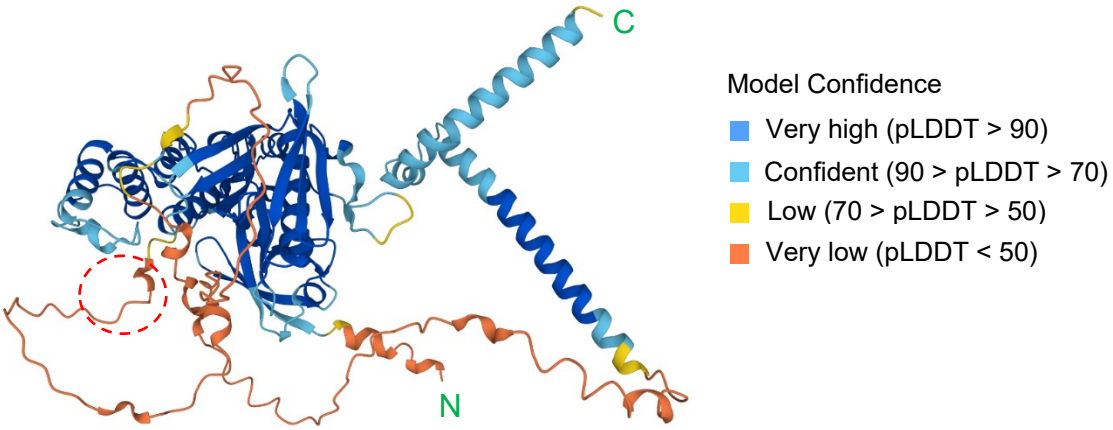

B

FERM domain (AA 21-354)

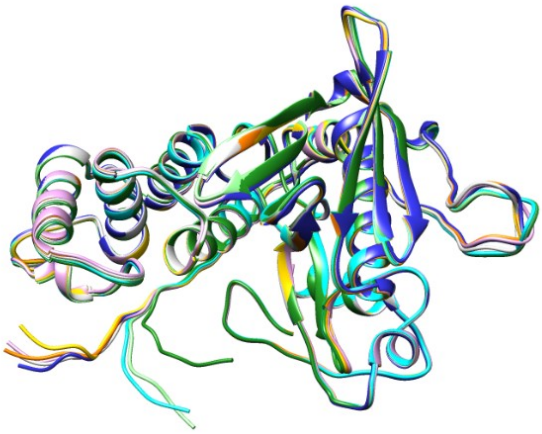

C

The AA 495-564 region

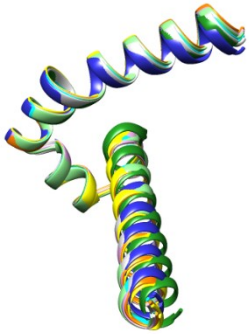

D

FRMD5	RMSD score (Å)	
	FERM domain (AA 21-354)	The AA 495-564 region
Ref	0	0
p.Phe114Leu	3.18	1.26
p.Ser351Gly	2.69	0.71
p.Ser351Arg	0.47	0.92
p.Cys352Arg	2.52	0.49
p.Ser354Pro	1.83	0.39
p.Ser349Arg	0.40	0.76
p.Tyr546Cys	0.62	1.06

Figure S5. Structural characterization of FRMD5 variants

(A-C) Predicted structures of FRMD5 reference (A) and variants (B-C) based on AlphaFold top predicted models. (A) The model confidence is shown in different colors. AlphaFold produces a per-residue confidence score (pLDDT) between 0 and 100. Some regions below 50 pLDDT may be unstructured in isolation. Note that FERM domain (AA 21-343) and the AA 495-564 region are confident (pLDDT > 70), while the other regions show low/very low confidence. The clustering region (AA 349-354) is highlighted in red dashed circle. The “N” and “C” label N-terminus and C-terminus of the protein, respectively. Structural alignment of FRMD5 variants with Ref in the FERM region (B) and the AA 495-564 region (C) was performed via UCSF Chimera[1]. (D) Root-mean-square deviation (RMSD) score for each variant compared to Ref is calculated using VMD software[2]. Two protein structures with an RMSD score of less than 3 Å would generally be considered to have no significant conformational changes[3].

Table S1: *In silico* characteristics of several *FRMD5* variants

***FRMD5* Variant (GRCh37)**	**Protein Change**	**Allele Frequency gnomAD**	**Number of Homozygotes gnomAD**	**MetaSVM**	**SIFT**	**POLYPHEN**	**REVEL Score**
15:44166583 C>T	p.Val405Met	0.0036	14	Tolerated	Tolerated	Benign	0.264
15:44165368 C>T	p.Gly511Asp	0.0035	5	Tolerated	Tolerated	Benign	0.209
15:44184197 C>T	p.Arg237Lys	0.0029	7	Tolerated	Tolerated	Benign	0.44
15:44166402 C>A	p.Ser465Ile	0.0016	4	Tolerated	Tolerated	Benign	0.249
15:44198035 G>A	p.Thr181Met	0.0014	6	Tolerated	Deleterious	Possibly Damaging	0.227
15:44166570 C>T	p.Arg409Gln	0.0008	1	Tolerated	Tolerated	Benign	0.188
15:44166159 T>C	p.Tyr546Cys	0	0	Damaging	Deleterious	Possibly Damaging	0.642

Table S2. Publicly available fly lines used in this study

Fly line	**Genotype**	**Source**
dFrmd$^{CRIMIC\text{-}TG4}$	*y^1 w^*; TI{GFP[3xP3.cLa]=CRIMIC.TG4.0}CG5022[CR00705-TG4.0]/SM6a*	BDSC #78994
Df	*w^{1118}; Df(2L)BSC208/CyO*	BDSC #9635
GR	*w^{1118}; Dp(2;3)GV-CH321-18A10, PBac{y[+mDint2] w[+mC]=GV-CH321-18A10}VK00031/TM3, Sb^1*	BDSC #89734
da-GAL4	*w^*; P{w[+mW.hs]=GAL4-da.G32}UH1, Sb^1/TM6B, Tb^1*	BDSC #55851
nub-GAL4	*w^*; P{w[nub.PK]=nub-GAL4.K}2*	BDSC #86108
UAS-mCherry.NLS	*w^*; P{w[+mC]=UAS-mCherry.NLS}3*	BDSC #38424
UAS-mCD8::RFP	*w^*; P{y[+t7.7] w[+mC]=10XUAS-IVS-mCD8::RFP}attP40*	BDSC #32219

Table S3: Primers used in this study.

Name	Species	Forward primer (5'-3')	Reverse primer (5'-3')	Assay
dFrmd	*Drosophila*	CTTCTCCTGGGGCACCAAAT	CTCGGCAAGCTGCTATATCTTAT	RT-PCR
rp49	*Drosophila*	TGTCCTTCCAGCTTCAAGATGACCATC	CTTGGGCTTGCGCATTTGTG	
FRMD5 c.340T>C (p.Phe114Leu)	*Homo sapiens*	TATTTAGTCCTCCTGCAGATC	CCTGGTTATTTCTTCTTTCAG	Mutagenesis
FRMD5 c.1045A>C *(*p.Ser349Arg*)*	*Homo sapiens*	GATGGTTCCCCGCCGGAGCTG	CCTGCTCTGTGTATTTCCGG	
FRMD5 c.1053C>G (p.Ser351Arg)	*Homo sapiens*	CCAGCCGGAGGTGTCCCTCCA	GAACCATCCCTGCTCTGTGTATTTCC	
FRMD5 c.1051A>G (p.Ser351Gly*)*	*Homo sapiens*	TCCCAGCCGGGGCTGTCCCTC	ACCATCCCTGCTCTGTGTATTTCCGG	
FRMD5 c.1054T>C (p.Cys352Arg)	*Homo sapiens*	CAGCCGGAGCCGTCCCTCCAT	GGAACCATCCCTGCTCTG	
FRMD5 c.1637A>G (p.Tyr546Cys)	*Homo sapiens*	CAATTCCACTGTCAATACTTTTGTCC	TTCAAACTCGGGGGTCTG	

Supplemental Material and Methods

Recruitment and sequencing of individuals

Six individuals were recruited through Maternal and Child Health Hospital of Hunan Province (proband 1 and 2) and Baylor Genetics Laboratories (proband 3, 4, 7 and 8). Proband 5 and 6 with severe undiagnosed developmental disorders were previously recruited by the Deciphering Developmental Disorders (DDD) Study[4], with the following information: Proband 5 (ID: 269740), https://www.deciphergenomics.org/ddd/research-variant/0dc53f15c5751a9b7d075050d10b1c96; Proband 6 (ID: 303400), https://www.deciphergenomics.org/ddd/research-variant/83738a9cbba51ea2fbb55855c05fd180. The procedures were followed in accordance with the ethical standards of the respective institutions. Proper informed consent was obtained from legal guardians of affected individuals. The DDD study has UK Research Ethics Committee approval (10/H0305/83, granted by the Cambridge South REC, and GEN/284/12 granted by the Republic of Ireland REC).

DNA sequencing methods

The exome sequencing (ES) were conducted on a clinical or research basis. For proband 1 and 2, Chigene performed trio ES followed by Sanger sequencing confirmation as previously described[5]. Baylor Genetics Laboratories performed ES and Sanger sequencing of probands 3, 4, 7 and 8, and the detailed sequencing and analysis protocols were published previously[6,7]. For proband 3, trio ES was performed and analyzed at Invitae. Briefly, genomic DNA obtained from the submitted sample was enriched for coding exons and adjacent splice junctions, generally exons +/- 10 base pairs, using a hybridization-based protocol. These regions were sequenced using Illumina technology to an average of ≥ 50x depth with minimum call depth of ≥ 20x. Reads were aligned to a reference sequence (GRCh37) and variants were identified using a custom-developed analysis tool. Identified variants were filtered and ranked using a proprietary algorithm, which considers known gene-phenotype associations, molecular variant

characteristics, zygosity, and population frequency, in the context of the individual's reported clinical presentation. This process is supported by an expertly curated gene-phenotype knowledgebase, as previously described[8]. Variants that may explain some or all of the individual's provided clinical indication were reviewed, interpreted, and reported according to ACMG guidelines[9]. Proband 5 and 6 with severe undiagnosed developmental disorders were recruited by the Deciphering Developmental Disorders (DDD) Study, and their samples were collected at the Wellcome Sanger Institute, where trio exome sequencing were applied to investigate the genetic causes of abnormal development. Likely diagnostic results are being reported to clinical team and their functional *de novo* mutations were confirmed in a public DDD research track in DECIPHER[4].

Fly stocks and genotypes

All flies used in this study were raised and maintained in plastic vials with standard cornmeal and molasses medium at room temperature, unless otherwise noted. Publicly available fly lines obtained from the Bloomington Drosophila Stock Center (BDSC) are listed in Table S2.

The *UAS-cDNA* lines were generated as described[10]. The *FRMD5* cDNA clone corresponding to GenBank transcript NM_032892.5, encoding isoform 2 (the longest isoform) is defined as the reference here. *FRMD5* variants were generated by Q5 site-directed mutagenesis (NEB). The fly *dFrmd* cDNA was obtained from DGRC GEO14235 (DGRC Stock 1658937; RRID: DGRC_1658937) and is defined as the wild type (WT). Primers for mutagenesis are listed in Table S3. All the human and fly cDNAs were cloned into pGW-UAS-HA.attB plasmid transgenic vector[11], and the pGW-UAS-Empty vector was used as the empty control[12]. The vectors were inserted into the VK33 (BDSC #24872) docking site by φC31 mediated transgenesis system[13].

Drosophila Behavioral Assays

Fly behavioral assays were performed as previously described[14]. For the heat shock assay, flies were transferred to an empty vial and submerged in a 42 °C water bath for 30 seconds.

The percentage of flies that are unable to keep an upright position was quantified. The time for flies to recover to a freely moving status was also measured. Flies that require more than 30 seconds to recover were recorded as 30 seconds.

ERG recording

ERG recordings were performed as previously described[15]. Briefly, flies were immobilized on a glass slide with glue. The recording electrode was placed on the corneal surface of the eye, and the reference electrode was inserted in the thorax. Flies were exposed to a series of light flashes for ERG recordings. For detailed methods of ERG recordings see Dolph et al., 2011[16].

Immunostaining

Immunostaining of fly larval and adult brains were performed as described[14]. Briefly, the samples were dissected in PBS and fixed with 4% Paraformaldehyde (PFA) in phosphate buffered saline (PBS) followed by blocking in PBS containing 0.2%Triton-X100 (0.2% PBST) with 5% normal goat serum. Primary antibodies used: rat anti-Elav deposited to the DSHB by Rubin G.M. (DSHB, 7E8A10; 1:500); mouse anti-Repo, deposited to the DSHB by Goodman C. (DSHB, 8D12; 1:50). Secondary antibodies used: goat anti-rat Alexa Fluor 647 (Jackson ImmunoResearch, 112-605-003; 1:500); goat anti-mouse Alexa Fluor 488 (Jackson ImmunoResearch, 115-545-062; 1:500). Samples were thoroughly washed with 0.2% PBST and mounted on a glass slide using Fluoromount-G (Southernbiotech, 0100-20). Samples were imaged with a confocal microscope (Leica SP8X), and images were processed using ImageJ.

Real-time (RT)-PCR

RT-PCR was performed as previously described[17] with several modifications. Total RNA was extracted by TRIzol Reagent (Thermo Fisher) using a standard protocol. Complementary DNA was made from 500-1000 ng of total RNA using All-In-One 5X RT MasterMix (abm #G592). RT-PCR reactions were performed with iTaq Universal SYBR Green Master Mix (BioRad

#1725120) and a BioRad C1000 Touch Cycler. *rp49* was used as an internal control gene. Primers were listed in Table S3.

Statistical Analysis

Statistical analysis was performed using GraphPad software (GraphPad Prism v9.0; GraphPad Software, USA). Data were analyzed by two-tailed unpaired t tests. Data are represented as mean + SEM, and n.s. (no significance) indicates $P > 0.05$; *$P < 0.05$; **$P < 0.01$; ***$P < 0.001$; ****$P < 0.0001$.

Supplemental Acknowledgments

We thank the probands and families for agreeing to participate in this study. We thank Ms. Hongling Pan for transgenic fly lines. We thank Hongjie Li, Oguz Kanca, Yiming Zheng and Meisheng Ma for their discussions and suggestions. We thank the Bloomington Drosophila Stock Center (BDSC) for numerous stocks, and Drosophila Genomics Resource Center (DGRC, supported by NIH Grant 2P40OD010949) for the fly cDNA clone. We thank the Chigene (Beijing) Translational Medicine Research Center Co. Ltd. for the technical support. This work was supported by the Howard Hughes Medical Institute (HHMI), the Huffington Foundation, and the Jan and Dan Duncan Neurological Research Institute at Texas Children's Hospital to H.J.B. Further support was obtained from The Office of Research Infrastructure Programs of the NIH (R24 OD022005 and R24 OD031447) to H.J.B. Research reported in this publication was also supported by the Eunice Kennedy Shriver National Institute of Child Health & Human Development of the National Institutes of Health (NIH) under award number P50HD103555 for use of the Neurovisualization core facilities. The content is solely the responsibility of the authors and does not necessarily represent the official views of the NIH. We thank the Deciphering Developmental Disorders (DDD) study for the referral of two probands. The DDD study presents independent research commissioned by the Health Innovation Challenge Fund [grant number HICF-1009-003]. This study makes use of DECIPHER

(https://www.deciphergenomics.org), which is funded by Wellcome [grant number 223718/Z/21/Z]. See Nature PMID: 25533962 or www.ddduk.org/access.html for full acknowledgement. This study makes use of data generated by the DECIPHER community. A full list of centres who contributed to the generation of the data is available from https://deciphergenomics.org/about/stats and via email from contact@deciphergenomics.org. Funding for the DECIPHER project was provided by Wellcome. Those who carried out the original analysis and collection of the Data bear no responsibility for the further analysis or interpretation of the data. We thank AlphaFold for structural predictions. The molecular graphics and analyses were performed with UCSF Chimera, developed by the Resource for Biocomputing, Visualization, and Informatics at the University of California, San Francisco, with support from NIH P41-GM103311.

Supplemental References

1. Pettersen, E.F., Goddard, T.D., Huang, C.C., Couch, G.S., Greenblatt, D.M., Meng, E.C., and Ferrin, T.E. (2004). UCSF Chimera--a visualization system for exploratory research and analysis. J. Comput. Chem. *25*, 1605-1612.
2. Humphrey, W., Dalke, A., and Schulten, K. (1996). VMD: visual molecular dynamics. J. Mol. Graph. *14*, 33-38, 27-38.
3. Reva, B.A., Finkelstein, A.V., and Skolnick, J. (1998). What is the probability of a chance prediction of a protein structure with an rmsd of 6 A? Fold Des *3*, 141-147.
4. Deciphering Developmental Disorders, S. (2015). Large-scale discovery of novel genetic causes of developmental disorders. Nature *519*, 223-228.
5. Huang, Y., Ma, M., Mao, X., Pehlivan, D., Kanca, O., Un-Candan, F., Shu, L., Akay, G., Mitani, T., Lu, S., et al. (2022). Novel dominant and recessive variants in human ROBO1 cause distinct neurodevelopmental defects through different mechanisms. Hum. Mol. Genet. *31*, 2751-2765.
6. Yang, Y., Muzny, D.M., Reid, J.G., Bainbridge, M.N., Willis, A., Ward, P.A., Braxton, A., Beuten, J., Xia, F., Niu, Z., et al. (2013). Clinical whole-exome sequencing for the diagnosis of mendelian disorders. N. Engl. J. Med. *369*, 1502-1511.
7. Vetrini, F., D'Alessandro, L.C., Akdemir, Z.C., Braxton, A., Azamian, M.S., Eldomery, M.K., Miller, K., Kois, C., Sack, V., Shur, N., et al. (2016). Bi-allelic Mutations in PKD1L1 Are Associated with Laterality Defects in Humans. Am. J. Hum. Genet. *99*, 886-893.
8. Clark, M.M., Hildreth, A., Batalov, S., Ding, Y., Chowdhury, S., Watkins, K., Ellsworth, K., Camp, B., Kint, C.I., Yacoubian, C., et al. (2019). Diagnosis of genetic diseases in seriously ill children by rapid whole-genome sequencing and automated phenotyping and interpretation. Sci. Transl. Med. *11,* eaat6177.
9. Richards, S., Aziz, N., Bale, S., Bick, D., Das, S., Gastier-Foster, J., Grody, W.W., Hegde, M., Lyon, E., Spector, E., et al. (2015). Standards and guidelines for the

interpretation of sequence variants: a joint consensus recommendation of the American College of Medical Genetics and Genomics and the Association for Molecular Pathology. Genet. Med. *17*, 405-424.
10. Harnish, J.M., Deal, S.L., Chao, H.T., Wangler, M.F., and Yamamoto, S. (2019). In Vivo Functional Study of Disease-associated Rare Human Variants Using Drosophila. J. Vis. Exp., e59658.
11. Bischof, J., Bjorklund, M., Furger, E., Schertel, C., Taipale, J., and Basler, K. (2013). A versatile platform for creating a comprehensive UAS-ORFeome library in Drosophila. Development *140*, 2434-2442.
12. Goodman, L.D., Cope, H., Nil, Z., Ravenscroft, T.A., Charng, W.L., Lu, S., Tien, A.C., Pfundt, R., Koolen, D.A., Haaxma, C.A., et al. (2021). TNPO2 variants associate with human developmental delays, neurologic deficits, and dysmorphic features and alter TNPO2 activity in Drosophila. Am. J. Hum. Genet. *108*, 1669-1691.
13. Venken, K.J., He, Y., Hoskins, R.A., and Bellen, H.J. (2006). P[acman]: a BAC transgenic platform for targeted insertion of large DNA fragments in D. melanogaster. Science *314*, 1747-1751.
14. Lu, S., Hernan, R., Marcogliese, P.C., Huang, Y., Gertler, T.S., Akcaboy, M., Liu, S., Chung, H.L., Pan, X., Sun, X., et al. (2022). Loss-of-function variants in TIAM1 are associated with developmental delay, intellectual disability, and seizures. Am. J. Hum. Genet. *109*, 571-586.
15. Jaiswal, M., Haelterman, N.A., Sandoval, H., Xiong, B., Donti, T., Kalsotra, A., Yamamoto, S., Cooper, T.A., Graham, B.H., and Bellen, H.J. (2015). Impaired Mitochondrial Energy Production Causes Light-Induced Photoreceptor Degeneration Independent of Oxidative Stress. PLoS Biol. *13*, e1002197.
16. Dolph, P., Nair, A., and Raghu, P. (2011). Electroretinogram recordings of Drosophila. Cold Spring Harb. Protoc. *2011*, pdb.prot5549.
17. Accogli, A., Lu, S., Musante, I., Scudieri, P., Rosenfeld, J.A., Severino, M., Baldassari, S., Iacomino, M., Riva, A., Balagura, G., et al. (2022). Loss of Neuron Navigator 2 Impairs Brain and Cerebellar Development. Cerebellum. 10.1007/s12311-022-01379-3